Collective Effects in Polariton Chemistry and Photophysics

Wenxiang Ying,[1] M. Elious Mondal,[1] Eric R. Koessler,[1] Sebastian Montillo Vega,[1] and Pengfei Huo[1,2,3,a)]
[1)] *Department of Chemistry, University of Rochester, Rochester, New York, 14627, USA*
[2)] *The Institute of Optics, Hajim School of Engineering, University of Rochester, Rochester, NY 14627, USA*
[3)] *Center for Coherence and Quantum Optics, University of Rochester, Rochester, New York 14627, USA*

(Dated: 1 December 2025)

Coupling molecules to the quantized radiation field inside an optical cavity creates a set of new photon-matter hybrid states, so-called polaritons. Recent experiments have demonstrated that molecular polaritons could lead to modifications of excited-state dynamics and spectroscopy, photochemistry, and ground-state chemical reactivities. We review the fundamental theory of molecular polaritons under collective light-matter coupling, where many molecules are simultaneously coupled to the cavity mode. Our discussions are based on model systems that effectively capture the essential physics of experiments, allowing one to obtain analytic theories and valuable insights into the microscopic mechanisms in polariton dynamics and spectroscopy, photochemistry, and vibrational strong coupling modified chemistry.

I. INTRODUCTION

Coupling molecules to quantized radiation field inside an optical microcavity (Fig. 1A) creates a set of new photon-matter hybrid states, these hybrid polariton states arise from the superposition between molecular states (electronic or vibrational excitation) and the cavity photon Fock states (photonic excitation) – so-called **polaritons**[1]. These polariton states have delocalized excitations among molecules and cavity modes. The formation of polariton states and their subsequent dynamics are considered key to many crucial phenomena, such as modifying chemical reactivities[1–5] and vibrational energy transfer[6–10], inducing changes in electron transfer[11–16] and photo-induced charge transfer[17], hot electron cooling dynamics and photoluminescence in nanomaterials[18–21], exciton transport[22–29] and excitation energy transfer[30–32], and so on, presenting a significant opportunity for innovation in material and energy science, quantum information platforms. For example, it is proposed that exciton-polaritons can be used for analog quantum simulation[33] and quantum computing[34].

There are two main regimes for polariton chemistry. One is related to electronic (excitonic) strong coupling (ESC) and photochemistry[3,35,36], operating under an external laser field to initiate photochemistry. The resulting hybrid electronic/excitonic-photonic states are usually referred as to exciton-polaritons. The other is vibrational strong coupling (VSC) and the change of ground-state reactivities[37–40], operating under the "dark condition" without any external laser pumping. The resulting hybrid molecular vibrational-photonic states are usually referred as to vibration polaritons.

Meanwhile, the light-matter hybrid states decay over time due to exciton-phonon coupling (vibrational environment of each molecule) and cavity losses, causing polariton relaxation and decoherence, which has interesting consequences on polariton dynamics and spectra. To take the polariton decay effects into account, a minimal model Hamiltonian that describes polariton formation in the single excitation subspace is expressed as[1,41,42]

$$\hat{\mathcal{H}} = \begin{bmatrix} \hbar\omega_{\rm c} - i\kappa/2 & \hbar\sqrt{N}g_{\rm c} \\ \hbar\sqrt{N}g_{\rm c} & \hbar\omega_0 - i\Gamma/2 \end{bmatrix}, \tag{1}$$

where $\omega_{\rm c}$ is the cavity frequency, ω_0 is the exciton frequency, $g_{\rm c}$ is the single molecule light-matter coupling strength, N is the number of molecules coupled to the cavity, κ is the cavity loss rate, and Γ is the exciton broadening. There are also $N-1$ dark states (see Eq. 10) which do not contain photonic character and are not included in Eq. 1. Furthermore, this description of polariton decay by adding an imaginary term is phenomenological and has certain limitations[43]. For example, it fails to account for polaritonic effects that arise from the polaron decoupling effect (see Section II E). A microscopic description of polariton decay can be reached by using the Holstein-Tavis-Cummings Hamiltonian (see Section II A), being more complete and does not miss important physics.

Under the resonant condition ($\omega_{\rm c} = \omega_0$), diagonalizing the Hamiltonian in Eq. 1 leads to the following complex eigenvalues[41,42,44], $E_\pm = \hbar(\omega_0+\omega_{\rm c})/2 - i(\kappa+\Gamma)/4 \pm \sqrt{N\hbar^2 g_{\rm c}^2 - (\kappa-\Gamma)^2/16}$, where E_+ and E_- are for the upper polariton (UP) and the lower polariton (LP), respectively, whose real part corresponds to the energy of the polariton states, and imaginary part corresponds to the broadening (or width of the spectral peak). The energy difference between these polariton states is the Rabi splitting, $\hbar\Omega_{\rm R} = E_+ - E_-$. The strong coupling condition is typically defined as $\hbar\Omega_{\rm R} > (\kappa+\Gamma)/2$, such that one can observe the splitting of the peaks in spectral measurements. In the presence of energy disorders (molecular transitions occur at different frequencies as a results of their local environments), recent the-

[a)] Electronic mail: pengfei.huo@rochester.edu

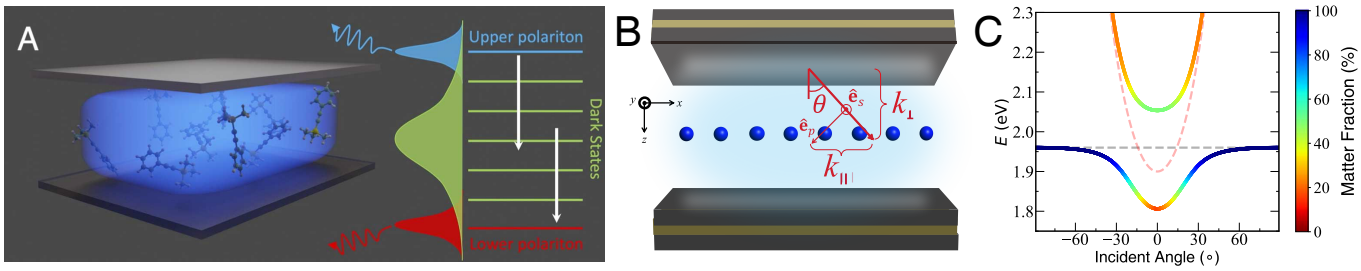

FIG. 1. Schematics of collective light-matter coupling inside a Fabry-Pérot cavity. (**A**) Schematic of molecules collectively coupled inside the cavity, forming upper polariton (UP), dark states (DS), and lower polariton (LP) states. (**B**) A simplified model of exciton sites coupled to photonic modes with $k_\parallel$. (**C**) Polariton dispersion relation, generated from the hybridization of the photonic dispersion (pink dashed line) and excitonic dispersion (black dashed line). The polariton dispersion is color-coded by its photonic character, with red for pure photonic character and blue for pure excitonic character. Panels (**B**) and (**C**) were adapted with permission from Ref. 29.

oretical work[45] suggests that delocalization of polariton states requires the collective light-matter coupling strength $\hbar\sqrt{N}g_{\rm c}$ to exceed four times the standard deviation of the energy disorder linewidth, in addition to just observe the Rabi splitting. Most experiments operate under the collective light-matter coupling regime, where the cavity mode interacts simultaneously with a large ensemble of molecules ($N \gg 1$), giving rise to a sizable Rabi splitting $\hbar\Omega_{\rm R} \propto \hbar\sqrt{N}g_{\rm c}$. Typical values of N have been estimated to be in the range of $N \approx 10^3 \sim 10^6$ per cavity mode for ESC[18,21] and $N \approx 10^6 \sim 10^{12}$ per cavity mode for VSC[46]. In experiments, the Rabi splitting is often in the range of $\hbar\Omega_{\rm R} \approx 50 \sim 420$ meV for ESC[18], and $\hbar\Omega_{\rm R} \approx 38 \sim 180$ cm^{-1}[37,40,47] for VSC. For matter optical transition frequency, typical values are $\hbar\omega_0 \approx 2$ eV for ESC and $\hbar\omega_0 \approx 800 \sim 3600$ cm^{-1} for VSC.

It is well understood how this collective light-matter coupling strength $\hbar\sqrt{N}g_{\rm c}$ impacts optical properties (such as polariton linear absorption spectra). However, how this collective light-matter coupling would impact polariton photochemistry[5] and VSC chemistry[48,49] remains elusive, and there are no well-accepted mechanisms. Many open questions are yet to be resolved, including (i) How can a weak coupling strength per molecule $g_{\rm c}$ change chemistry and lead to collective effects? (ii) How can delocalized excitations among molecules and cavity modes impact *local* chemical reactions (*i.e.* the intrinsic reaction mechanism of a single molecule in the absence of a cavity)? (iii) How does the dense manifold of dark exciton states impact polariton chemistry? Intuitively, one may expect that the collective quantity $\hbar\Omega_{\rm R}$ should manifest in the rate constant of these reactions when coupled to the cavity.

This review provides a summary of collective effects in polariton chemistry and photophysics due to the nature of collective light-matter coupling, and address the nature of the many controversies in this field (both experimental and theoretical). In Section II, we provide a theoretical overview of collective light-matter interaction Hamiltonians, with diabatic or adiabatic representations of polariton states, and introduce the polaron decoupling effect. In Section III, we discuss some simple rate theories for polariton relaxation dynamics, decoherence, and linear spectra lineshape. In Section IV, we present a collective mechanism for the rate enhancement of polariton-mediated electron transfer (PMET) reactions. In Section V, we discuss recent theoretical developments that provide insights into the resonant rate suppression effects in VSC.

II. THEORETICAL MODELS

In typical experiments, molecule ensembles are collectively coupled to many cavity modes (Fig. 1B) that satisfy a certain dispersion relation (Fig. 1C). For Fabry-Pérot (FP) cavities (see schematics in Fig. 1A) with refractive index $n_{\rm c}$, the dispersion is

$$\hbar\omega_{\mathbf{k}}(k_\parallel) = \frac{\hbar c}{n_{\rm c}}\sqrt{k_\perp^2 + k_\parallel^2} = \frac{\hbar c}{n_{\rm c}} k_\perp \sqrt{1+\tan^2\theta}, \qquad (2)$$

where c is the speed of light, $\hbar k_\parallel$ is the in-plane photonic momentum, and $\hbar k_\perp$ is the photonic momentum along the quantized direction. The angle θ indicates the direction of $\mathbf{k}$ relative to the normal direction of the cavity mirror (see Fig. 1B). When $k_\parallel = 0$, the photon frequency is $\hbar\omega_{\rm c} \equiv \hbar\omega_{\mathbf{k}}(k_\parallel = 0) = \hbar c k_\perp / n_{\rm c}$.

A general model Hamiltonian that describes N non-interacting identical two-level molecular excitons coupled to many cavity modes (Eq. 2) can be expressed as[1]

$$\hat{H} = \sum_{n=1}^{N} \hbar\omega_0 \hat{\sigma}_n^+ \hat{\sigma}_n^- + \sum_{\mathbf{k}} \hbar\omega_{\mathbf{k}} \left(\hat{a}_{\mathbf{k}}^\dagger \hat{a}_{\mathbf{k}} + \frac{1}{2}\right) + \sum_{n=1}^{N}\sum_{\mathbf{k}} \hbar g_{n\mathbf{k}} \left(\hat{a}_{\mathbf{k}}^\dagger \hat{\sigma}_n^- e^{-i\mathbf{k}\cdot\mathbf{r}_n} + \hat{a}_{\mathbf{k}} \hat{\sigma}_n^+ e^{i\mathbf{k}\cdot\mathbf{r}_n}\right), \qquad (3)$$

where we ignored the dipole self-energy[1] and assume the rotating wave approximation[1] (ignoring terms such as

$\hat{a}^\dagger\hat{\sigma}_n^+$ and $\hat{a}\hat{\sigma}_n^-$ that do not conserve energy). In Eq. 3, $\hat{\sigma}_n^+ = |e_n\rangle\langle g_n|$ ($\hat{\sigma}_n^- = |g_n\rangle\langle e_n|$) is the creation (annihilation) operator of the $n_{\rm th}$ exciton, whose ground and excited states are $|g_n\rangle$ and $|e_n\rangle$, respectively, with an excitation energy ω_0 (for $|g_n\rangle \to |e_n\rangle$ transition). And the position of the $n_{\rm th}$ exciton is $\mathbf{r}_n$. The transition dipole operator is $\hat{\boldsymbol{\mu}}_n = \boldsymbol{\mu}_{eg}(\hat{\sigma}_n^+ + \hat{\sigma}_n^-)$, assuming all excitons have the same dipole moment. Furthermore, $\hat{a}_{\mathbf{k}}$ and $\hat{a}_{\mathbf{k}}^\dagger$ are the photonic field annihilation and creation operators for mode $\mathbf{k}$ whose frequency is $\omega_{\mathbf{k}}$. The anisotropic light-matter coupling strength is $g_{n\mathbf{k}}$. A detailed derivation of the Hamiltonian in Eq. 3 can be found in Ref. 1.

Based on Eq. 3, a simplified description can be reached by setting $\mathbf{r}_n = 0$ for all molecules n when the molecular system size is much smaller than $c/(2\pi\omega_0)$, known as the long-wavelength approximation[1]. Further taking a single radiation field mode as a cavity mode and assume a uniform coupling strength $g_{n\mathbf{k}} = g_{\rm c}$, one reaches to the celebrated Tavis-Cummings (TC) model[50,51], see Eq. 4 below, being a minimal theoretical model to describe collective light-matter coupling. The TC Hamiltonian can be analytically diagonalized in the single excitation subspace, leading to two polariton states and $N-1$ dark states, see Section II B.

Next, polariton relaxation and decoherence (which prove to be important in chemistry) are accounted for by incorporating exciton-phonon couplings into the TC model, leading to the Holstein-Tavis-Cummings (HTC) model[1,18,52–54], see Section II A below. The HTC model has been widely used in the study of exciton-polaritons in molecular aggregates[52,53,55], and in polariton condensation and lasing[56,57], in which the exciton-phonon couplings are included in the Hamiltonian using a system-bath model[58], corresponding to a microscopic description of molecular dissipation and in contrast to the oversimplified non-Hermitian effective Hamiltonian in Eq. 1. We focus on the HTC type of Hamiltonian throughout this review, while the details depend on the problem studied, *i.e.*, more complicated reaction coordinates are considered when studying polariton modified chemistry (PMET and VSC).

A. The Holstein-Tavis-Cummings Hamiltonian

We consider the single-mode HTC Hamiltonian expressed in the form of a system-bath model[58] as $\hat{H}_{\rm HTC} = \hat{H}_{\rm S} + \hat{H}_{\rm B} + \hat{H}_{\rm SB} + \hat{H}_{\rm loss}$.

1. Molecules-Cavity Interactions

The system term $\hat{H}_{\rm S}$ consists of the excitonic degree of freedom (DOF) of the molecules and the photonic DOF of the cavity,

$$\hat{H}_{\rm S} = \sum_{n=1}^{N} \hbar\omega_0 \hat{\sigma}_n^+\hat{\sigma}_n^- + \hbar\omega_{\rm c}\left(\hat{a}^\dagger\hat{a} + \frac{1}{2}\right) + \hbar g_{\rm c}\sum_{n=1}^{N}\left(\hat{a}^\dagger\hat{\sigma}_n^- + \hat{a}\hat{\sigma}_n^+\right), \tag{4}$$

which is the TC Hamiltonian[50,51]. The second term in Eq. 4 describes a cavity mode of frequency $\omega_{\rm c}$, and the third is the light-matter (exciton-photon) interaction. The light-matter coupling strength is $g_{\rm c} = \sqrt{\omega_{\rm c}/(2\hbar\epsilon\mathcal{V})}\ \hat{\mathbf{e}}\cdot\boldsymbol{\mu}_{eg}$, where $\hat{\mathbf{e}}$ is the cavity field polarization direction, ϵ is the permittivity inside the cavity (for vacuum, $\epsilon = \epsilon_0$), and $\mathcal{V}$ is the effective cavity quantization volume. In Eq. 4, we assume identical excitons with no inhomogeneous energy or orientational dipole disorder.

2. System-Bath Hamiltonian

The bath Hamiltonian is $\hat{H}_{\rm B} = \sum_{\alpha,n}\hbar\omega_\alpha\hat{b}_{\alpha,n}^\dagger\hat{b}_{\alpha,n}$, where $\hat{b}_{\alpha,n}$ ($\hat{b}_{\alpha,n}^\dagger$) is the annihilation (creation) operator for the $\alpha_{\rm th}$ phonon mode on $n_{\rm th}$ exciton of frequency ω_α. Furthermore, the excitons interact with the phonons according to the Holstein-like interaction $\hat{H}_{\rm SB} = \sum_n \hat{\sigma}_n^+\hat{\sigma}_n^- \otimes \sum_\alpha c_\alpha(\hat{b}_{\alpha,n} + \hat{b}_{\alpha,n}^\dagger)$, where c_α is the coupling strength of the $\alpha_{\rm th}$ phonon with the $n_{\rm th}$ exciton, sampled from a spectral density $J_n(\omega) = J(\omega) = \frac{\pi}{\hbar}\sum_\alpha c_\alpha^2\delta(\omega-\omega_\alpha)$, where $\lambda = (1/\pi)\int_0^{+\infty} d\omega\ J(\omega)/\omega = \sum_\alpha c_\alpha^2/(\hbar\omega_\alpha)$ is the reorganization energy. For model parameterization, atomistic simulations of real molecular systems can be used to construct $J(\omega)$ and obtain λ[59].

3. Cavity Loss Dynamics

The lifetime of the cavity mode $\tau_{\rm c}$ is finite, due to its coupling with the far-field photon modes outside the cavity. This can be modeled by $\hat{H}_{\rm loss} = \sum_k \hbar\omega_k\hat{b}_k^\dagger\hat{b}_k + (\hat{a}^\dagger + \hat{a}) \otimes \sum_k \hbar g_k(\hat{b}_k^\dagger + \hat{b}_k)$, where $\hat{b}_k^\dagger$ ($\hat{b}_k$) is the raising (lowering) operator for $k_{\rm th}$ far-field mode. The interactions between the cavity mode and the far-field modes can be described by the Gardiner-Collett interaction Hamiltonian[60–62], where the broad range of the far-field frequencies leads to short correlation time, justifying the Markovian treatment of loss and giving rise to the Lindblad master equation[63] $d\hat{\rho}_{\rm S}/dt = -\frac{i}{\hbar}\left[\hat{H}_{\rm S}, \hat{\rho}_{\rm S}\right] + \frac{\kappa}{\hbar}(\hat{a}\hat{\rho}_{\rm S}\hat{a}^\dagger - \frac{1}{2}\{\hat{a}^\dagger\hat{a}, \hat{\rho}_{\rm S}\})$, where $\hat{\rho}_{\rm S}$ is the reduced density matrix associated with $\hat{H}_{\rm S}$, and $\kappa/\hbar \equiv \tau_{\rm c}^{-1}$ is the cavity loss rate, which is experimentally related to the cavity quality factor, $\mathcal{Q} = \omega_{\rm c}\tau_{\rm c}$.

B. Polariton States and Dark States

For the Hamiltonian in Eq. 4, the ground state is $|\mathrm{G},0\rangle = |g_1\rangle \otimes ... \otimes |g_N\rangle \otimes |0\rangle$ and the first excitation subspace is spanned by

$$\begin{aligned} |\mathrm{G},1\rangle &= |g_1\rangle \otimes ... \otimes |g_N\rangle \otimes |1\rangle \\ |\mathrm{E}_n,0\rangle &= |g_1\rangle \otimes ...|e_n\rangle ... \otimes |g_N\rangle \otimes |0\rangle, \end{aligned} \tag{5}$$

where $|0\rangle$, $|1\rangle$ are the vacuum and one photon Fock states, respectively. One can define a collective "bright" excitonic state $|\mathrm{B},0\rangle = \frac{1}{\sqrt{N}}\sum_{n=1}^{N}|\mathrm{E}_n,0\rangle$, which carries the optical transition dipole from the ground state, $\langle \mathrm{G},0|\hat{\mu}|\mathrm{B},0\rangle = \sum_{n=1}^{N}(\mu_{eg}/\sqrt{N}) = \sqrt{N}\mu_{eg}$. Note that we have assumed that the dipoles are all aligned to the cavity field polarization, so that $\hat{\mathbf{e}}\cdot\boldsymbol{\mu}_{eg} = \mu_{eg}$. The light-matter interactions cause the hybridization of $|\mathrm{B},0\rangle$ and $|\mathrm{G},1\rangle$, leading to two bright polariton eigenstates (of $\hat{H}_\mathrm{S}$),

$$\begin{aligned} |+\rangle &= \cos\Theta \cdot |\mathrm{B},0\rangle + \sin\Theta \cdot |\mathrm{G},1\rangle \\ |-\rangle &= -\sin\Theta \cdot |\mathrm{B},0\rangle + \cos\Theta \cdot |\mathrm{G},1\rangle, \end{aligned} \tag{6}$$

where the mixing angle is $\Theta = \frac{1}{2}\tan^{-1}[2\sqrt{N}g_\mathrm{c}/(\Delta_\omega)]$ with $\Theta \in [0, \frac{\pi}{2})$, and the light-matter detuning $\Delta_\omega \equiv \omega_\mathrm{c} - \omega_0$. At resonance, $\Delta_\omega = 0$ and $\Theta = \pi/4$. Note that Θ can also be expressed in terms of the Hopfield coefficients[1,44,64],

$$\begin{aligned} |C|^2 = \sin^2\Theta &= \frac{1}{2}\Big[1 + \frac{\Delta_\omega}{\sqrt{\Delta_\omega^2 + 4Ng_\mathrm{c}^2}}\Big], \\ |X|^2 = \cos^2\Theta &= \frac{1}{2}\Big[1 - \frac{\Delta_\omega}{\sqrt{\Delta_\omega^2 + 4Ng_\mathrm{c}^2}}\Big]. \end{aligned} \tag{7}$$

The corresponding eigenfrequencies are

$$\omega_\pm = \frac{1}{2}(\omega_0 + \omega_\mathrm{c}) \pm \frac{1}{2}\sqrt{\Delta_\omega^2 + 4Ng_\mathrm{c}^2}, \tag{8}$$

with a schematic illustration in Fig. 2A.

C. Rabi Splitting Ω_R is a Collective Quantity.

The Rabi splitting is

$$\hbar\Omega_\mathrm{R} = \hbar\omega_+ - \hbar\omega_- = \hbar\sqrt{\Delta_\omega^2 + 4Ng_\mathrm{c}^2}, \tag{9}$$

At resonance ($\Delta_\omega = 0$), Eq. 9 becomes $\Omega_\mathrm{R} = 2\sqrt{N}g_\mathrm{c}$ which makes $\hbar\Omega_\mathrm{R}$ a *collective quantity*. Experimentally, even a small g_c can result in a large $\hbar\Omega_\mathrm{R}$ due to very large N.

Apart from the two polariton eigenstates in Eq. 6, $\hat{H}_\mathrm{S}$ also has additional $N-1$ *degenerate* eigenstates in the first excitation manifold (Eq. 5), with eigenenergies $\hbar\omega_0$ and are commonly expressed in the "delocalized" Fourier basis[1,50,65],

$$|\mathrm{D}_k\rangle = \frac{1}{\sqrt{N}}\sum_{n=1}^{N}\exp\Big(-2\pi i\frac{nk}{N}\Big)|\mathrm{E}_n,0\rangle, \tag{10}$$

where $k \in \{1, \cdots, N-1\}$. These are commonly referred to as "dark states" because of their optically dark nature, $\langle \mathrm{G},0|\hat{\mu}|\mathrm{D}_k\rangle = (\mu_{eg}/\sqrt{N}) \cdot \sum_{n=1}^{N}\exp(-2\pi i\,\frac{nk}{N}) = 0$.

Under the polariton basis, the HTC Hamiltonian becomes purely diagonal, $\hat{H}_\mathrm{S} = \hbar\omega_+|+\rangle\langle+| + \hbar\omega_-|-\rangle\langle-| + \hbar\omega_0\sum_{k=1}^{N-1}|\mathrm{D}_k\rangle\langle\mathrm{D}_k|$. Using discrete Fourier transform for the phonon operators, $\hat{b}_{\alpha,k} = \frac{1}{\sqrt{N}}\sum_{n=1}^{N}\exp\big(2\pi i\frac{nk}{N}\big)\hat{b}_{\alpha,n}$, the bath Hamiltonian is $\hat{h}_\mathrm{B} = \sum_{\alpha,k}\hbar\omega_\alpha\hat{b}_{\alpha,k}^\dagger\hat{b}_{\alpha,k}$, and the system-bath Hamiltonian becomes[66,67]

$$\hat{H}_\mathrm{SB} = \sum_{\eta\nu,kk'}\xi_{\eta k}\cdot\xi_{\nu k'}|\eta_k\rangle\langle\nu_{k'}| \otimes \sum_\alpha \frac{c_\alpha}{\sqrt{N}}(\hat{b}_{\alpha,k-k'} + \hat{b}_{\alpha,k'-k}^\dagger), \tag{11}$$

where the state labels $\eta,\nu \in \{+,-\}$ for $k=0$ (bright) while $\eta,\nu \equiv \mathrm{D}$ for $k \neq 0$ (dark). Furthermore, $\xi_{\eta k}$ is a state-dependent coefficient that characterizes the matter fraction of the polariton state, with $\xi_+ = \cos\Theta$ and $\xi_- = \sin\Theta$ for $k=0$, and $\xi_{\mathrm{D}k} = 1$ for $k \neq 0$. Note that $|\xi_\pm|^2$ are just the Hopfield coefficients in Eq. 7. From Eq. 11, one sees that transitions between eigenstates are mediated by phonons. In particular, $\langle \mathrm{D}_k|\hat{H}_\mathrm{SB}|+\rangle = \cos\Theta\cdot\sum_\alpha(c_\alpha/\sqrt{N})(\hat{b}_{\alpha,k} + \hat{b}_{\alpha,-k}^\dagger)$ and $\langle \mathrm{D}_k|\hat{H}_\mathrm{SB}|-\rangle = \sin\Theta\cdot\sum_\alpha(c_\alpha/\sqrt{N})(\hat{b}_{\alpha,-k} + \hat{b}_{\alpha,k}^\dagger)$ cause $|\pm\rangle \leftrightarrow |\mathrm{D}_k\rangle$ transitions.

D. Diabatic vs Adiabatic Representations of Polariton States

The polariton and dark states in Eq. 6 and Eq. 10 are defined in the absence of nuclear motion, as they are constructed from the photonic and electronic DOF with the nuclear configuration held fixed (*i.e.*, independent of $\{\hat{R}_{n,\alpha}\}$ or $\hat{b}_{\alpha,n}^\dagger + \hat{b}_{\alpha,n}$). These are often referred to as the *diabatic* polariton states, because they do not account for the dependence of polaritonic eigenstates on the nuclear coordinates. In this representation, the nuclear DOF act as a bath, leading to transitions between polariton and dark states through exciton-phonon interactions (see $\hat{H}_\mathrm{SB}$ in Eq. 11).

Alternatively, one can define the *adiabatic* polariton representation by treating the nuclear coordinates as parameters and diagonalizing the full electronic-photonic Hamiltonian at each fixed nuclear geometry $\mathbf{R} = \{R_{n,\alpha}\}$, *i.e.*, $\hat{H}_\mathrm{pl} = \hat{H} - \hat{T}_R$ (excluding nuclear kinetic energy), and solving $\hat{H}_\mathrm{pl}(\mathbf{R})|\Phi_k(\mathbf{R})\rangle = E_k(\mathbf{R})|\Phi_k(\mathbf{R})\rangle$. The resulting eigenstates $|\Phi_k(\mathbf{R})\rangle$ then include the influence of the nuclear environment, and the nuclear dynamics occurs on the polariton potential energy surfaces (PES), see Fig. 2B for example. In this picture, nonadiabatic couplings (also known as the derivative couplings), *i.e.*, terms such as $\langle\Phi_i(\mathbf{R})|\nabla_{n,\alpha}|\Phi_j(\mathbf{R})\rangle$ that originate from the bath nuclear momentum operator $\hat{P}_{n,\alpha} = -i\hbar\nabla_{n,\alpha}$, govern the transitions between adiabatic polariton states,

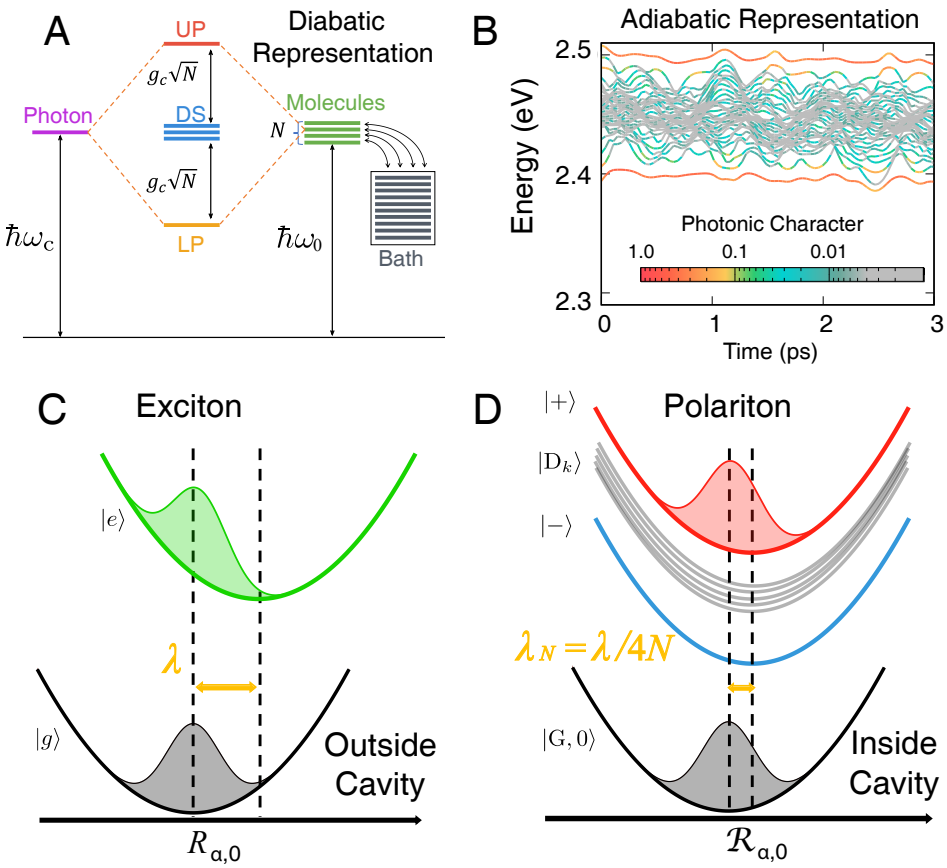

FIG. 2. Schematic of N excitons collectively coupled to a cavity mode, forming $N+1$ eigenstates (UP, LP and DS), under the (**A**) diabatic and (**B**) adiabatic representation, respectively. Panel (**C**) shows the ground state $|g\rangle$ PES (grey) and excited state $|e\rangle$ PES (green) with a Frank-Condon excited wavepacket when a bare molecular exciton is presented outside the cavity. Panel (**D**) shows the collective ground state $|\mathrm{G},0\rangle$ PES (grey) and UP $|+\rangle$ PES (red) with a Frank-Condon excited wavepacket when N molecules collectively couple to a cavity mode. The LP $|-\rangle$ PES (blue) and the DS $|\mathrm{D}_k\rangle$ PES (dark-grey) are also depicted. Panel (**A**) was adapted with permission from Ref. 66, copyright @ 2024 AIP Publishing. Panel (**B**) was adapted with permission from Ref. 18, copyright @ 2021 American Chemical Society.

and are responsible for energy transfer, decoherence, and relaxation.

The choice between these representations depends on the physical situation of interest. The diabatic picture is particularly convenient for describing transitions mediated by phonon baths (*e.g.*, using quantum master equation approaches[66,67]), while the adiabatic picture is useful for describing nuclear wavepacket dynamics[68–70] or semiclassical propagation[69–71] with nonadiabatic transitions. Importantly, these adiabatic dark states are no longer degenerate and no longer strictly "dark"[18], as their character depends on the local nuclear configurations $\mathbf{R} = \{R_{n,\alpha}\}$, see Fig. 2B. This lifting of degeneracy is shown crucial for understanding decoherence and energy flow between bright and dark manifolds.

E. Polaron Decoupling Effect

Herrera and Spano[52,53] demonstrated that a strong collective resonant coupling of a cavity field with N exciton transitions effectively decouples excitons from phonon interactions, as also confirmed experimentally[72]. To be specific, the exciton-phonon coupling strength c_α is re-scaled as $c_\alpha/\sqrt{N}$ for both the diagonal (Holstein coupling) and off-diagonal (Peierls coupling) terms associated with the bright states $|\pm\rangle$ (see Eq. 11). As such, the relative displacement caused by the α_{th} phonon on the $|\pm\rangle$ state with respect to $|\mathrm{G},0\rangle$ is given by[53] $\mathcal{R}_{\alpha,0} = R_{\alpha,0}/(2\sqrt{N})$ (at resonance), where $R_{\alpha,0} = \sqrt{2c_\alpha^2/(M_\alpha\hbar\omega_\alpha^3)}$ (with reduced mass $M_\alpha = 1$ a.u.). Thus, the effective reorganization energy for the $|\pm\rangle$ state becomes

$$\lambda_N = \frac{1}{2}\sum_\alpha M_\alpha\omega_\alpha^2\mathcal{R}_{\alpha,0}^2 = \frac{\lambda}{4N}, \tag{12}$$

which is $4N$ times smaller than outside the cavity case. When the Rabi oscillation period is shorter than vibrational time scales, excitons can exchange energy with the cavity mode multiple times before nuclei adapt to the excited state potential. For large N, the homogeneous reorganization energy approaches zero, so the equilibrium positions of the bright and ground state potentials align[52,53]. Using the shifted harmonic oscillator model[73], Fig. 2C illustrates the PES for both the ground ($|g\rangle$) and excited ($|e\rangle$) states of an isolated molecular exciton. Shown in grey, the ground state PES features a thermal wavepacket at equilibrium, which, when subjected to Franck-Condon (FC) excitation, causes the wavepacket to shift within the excited state (depicted in green) relative to the minima of its corresponding PES. Similarly, Fig. 2D depicts the effect of polaron decoupling. The polaritonic states, $|+\rangle$ (red) and $|-\rangle$ (blue), remain largely unshifted relative to the ground state, leading to the FC excited state wavepacket closely resembling the ground state thermal wavepacket. This significantly reduces the nonadiabatic force due to excited state PES shift (as seen for excitons) in wavepacket dynamics.

III. EXCITON-POLARITONS RELAXATION DYNAMICS AND SPECTRA

In this section, we review several analytic results derived from the HTC Hamiltonian that shed light on the fundamental properties of molecular polaritons under the collective coupling regime. There has been a broad spectrum of experimental studies on the excited state properties of exciton-polaritons[74–82]. Most of these experimental results have been well understood based on the current theoretical framework.

A. Polariton Relaxation Dynamics

Previous computational studies on the HTC model excited-state properties utilized various exact quantum dynamics methods[83–86], trajectory-based mixed-quantum-classical (MQC) methods[87,88]. Exploiting the symmetry and sparsity of $\hat{H}_{\rm S}$ can notably lower the scaling and computational costs for $(\hat{H}_{\rm S}+\hat{H}_{\rm SB})|\Psi(t)\rangle$, allowing direct simulations for HTC model with $N=10^6$, as detailed in Ref. 88. Exploiting the symmetry of the HTC Hamiltonian can bypass the need to explicitly simulate dynamics with large N. For example, by assuming uncorrelated excitons, the dynamics can be represented by a pair of mean-field equations of motion[89,90] for one excitonic and one photonic DOF, respectively. Another example is the collective dynamics using truncated equations (CUT-E) approach[91], which leverages the permutational symmetry of matter states to lower computational demands through an effective $1/N$ expansion[92].

On the other hand, the polariton relaxation dynamics can be well described by Fermi's golden rule (FGR) rate constants when the phonon bath coupling $\hat{H}_{\rm SB}$ can be treated perturbatively[66]. In particular, the $|\pm\rangle \to \{|{\rm D}_k\rangle\}$ transition rates are[66,93]

$$k_{+\to {\rm D}} = \frac{N-1}{\hbar N}\cdot(1+\cos 2\Theta)\cdot J(\omega_+-\omega_0)\cdot[\overline{n}(\omega_+-\omega_0)+1], \tag{13a}$$

$$k_{-\to {\rm D}} = \frac{N-1}{\hbar N}\cdot(1-\cos 2\Theta)\cdot J(\omega_0-\omega_-)\cdot\overline{n}(\omega_0-\omega_-), \tag{13b}$$

where $\bar{n}(\omega)=1/(e^{\beta\hbar\omega}-1)$ is the Bose-Einstein distribution function , $\beta=1/(k_{\rm B}T)$, and $k_{\rm B}$ is the Boltzmann constant. Starting from an arbitrary state in the dark states manifold (or even a statistical mixture of them), the $\{|{\rm D}_k\rangle\}\to|-\rangle$ transition rate is

$$k_{{\rm D}\to -} = \frac{1}{\hbar N}\cdot(1-\cos 2\Theta)\cdot J(\omega_0-\omega_-)\cdot\overline{n}(\omega_0-\omega_-). \tag{13c}$$

One sees that unlike $k_{\pm\to {\rm D}}$ (Eqs. 13a-b), $k_{{\rm D}\to -}$ does not include the $N-1$ degeneracy factor. This is because $|\pm\rangle\to\{|{\rm D}_k\rangle\}$ involves $N-1$ degenerate final states, while $\{|{\rm D}_k\rangle\}\to|-\rangle$ involves only $|-\rangle$ as the final state and does not acquire the $N-1$ factor. Hence, $\{|{\rm D}_k\rangle\}\to|-\rangle$ occurs much slower compared to $|\pm\rangle\to\{|{\rm D}_k\rangle\}$. In real experiments[6,7], dark excitons also decay via non-radiative relaxation, but the time scale is much longer than the polariton lifetime. Furthermore, the large $N-1$ degeneracy fold of the dark states manifold may also be interpreted from the entropy perspective[94], because Eq. 13b can be recasted as $k_{-\to {\rm D}}\approx\frac{1}{\hbar N}\cdot[1-\cos(2\Theta)]\cdot J(\omega_0-\omega_-)\cdot e^{-\beta[\hbar(\omega_0-\omega_-)-k_{\rm B}T\ln(N-1)]}$, such that one can define an effective entropy change $\Delta S=k_{\rm B}\ln(N-1)$ associated with the transition. Note that it differs from the thermodynamics entropy since $N-1$ is not the actual particle number but the degeneracy fold of the dark states manifold. When the dark states dominate the equilibrium population, it can be explained as the dark states manifold has a relatively lower free energy than the LP, with $\Delta\mathcal{F}=\hbar(\omega_0-\omega_-)-k_{\rm B}T\ln(N-1)\equiv\Delta E-T\Delta S<0$.

Note that the FGR expressions in Eq. 13 are based on an equilibrium assumption and ignore any transient non-equilibrium dynamics. A non-equilibrium version of these FGR rates of the quantum time-correlation function formalism can be derived[66], which are time-dependent and upon taking the long-time limit, reduce to the equilibrium FGR rate constants. These simple FGR rate constants in Eq. 13 offer insight into why simulating polariton relaxation dynamics with a reduced N and elevated $g_{\rm c}$ often succeeds, provided the Rabi splitting $\hbar\Omega_{\rm R}\propto\hbar\sqrt{N}g_{\rm c}$ stays constant. The key is that the relaxation rates in Eq. 13 are influenced by collective quantities ($\Omega_{\rm R}$ and N) instead of individual coupling strength $g_{\rm c}$.

B. Polariton Coherence Decay

The polaron decoupling effect[52,88,95,96] discussed in Section II E can protect overall quantum coherence from phonon coupling-induced decoherence, for both the single molecule strong coupling[97] and the collective coupling regime[88,93,98]. This has been confirmed with a prolonged beating off-diagonal signal in two-dimensional electronic spectroscopy (2DES) as shown in Ref. 99. Compared to the typical electronic coherence lifetime ($T_2 \sim$15 fs), the coherence lifetime of exciton polaritons can be extended to $\sim$100 fs at room temperature[93].

The polaritonic coherence can be characterized by the amplitude of $\rho_{+-}(t) = \langle +|\hat{\rho}_{\rm S}(t)|-\rangle$. Ref. 93 reveals that the primary decoherence mechanism is the population transfer from the bright to the dark states manifold as well as the cavity loss. Increasing $\Omega_{\rm R}$ prolongs the coherence lifetime due to the phonon bottleneck effect[19]. Under the $N \to \infty$ condition, transitions between bright polariton states are negligible. As such, the polariton coherence lifetime can be approximated as[93]

$$T_2^{-1} \approx \frac{1}{2}k_{+\to {\rm D}} + \frac{1}{2}k_{-\to {\rm D}} + \frac{1}{2}\tau_{\rm c}^{-1}, \tag{14}$$

where $k_{\pm\to {\rm D}}$ is expressed in Eqs. 13a-b, and $\tau_{\rm c}^{-1}$ is the cavity loss rate. For $\Delta_\omega \leqslant 0$, the rate $k_{-\to {\rm D}}$ can be ignored due to the uphill $|-\rangle \to \{|{\rm D}_k\rangle\}$ transition. For $\Delta_\omega > 0$, the LP is closer to the DS manifold than the UP, and both $k_{\pm\to {\rm D}}$ could have significant contributions. Eq. 14 predicts the fundamental scaling relation between T_2^{-1} with respect to N, $\sqrt{N}g_{\rm c}$, $\tau_{\rm c}$, and Δ_ω. For example, when $J(\omega)$ takes a Drude-Lorentz form, Eq. 14 suggests that $T_2^{-1} \propto (N-1)/(N^{3/2}g_{\rm c})$, which has been confirmed by numerical exact quantum dynamics simulations using the hierarchical equations of motion (HEOM) approach[93]. Furthermore, Eq. 14 predicts that there will be a turnover of T_2 as one changes the Δ_ω values[93]. These predictions can be experimentally checked with state-of-the-art 2DES measurements[99] that directly report off-diagonal beatings between the UP and the LP states. The prolonged polariton coherence at room temperature could potentially be useful for quantum information science applications[33,34].

C. Polariton Linear Absorption (LA) Spectra

The LA spectra can be directly computed from the Fourier transform of the dipole-dipole correlation function according to $\mathcal{A}(\omega) \propto \int_0^\infty dt\ \mathcal{A}(t)e^{i\omega t}$, where $\mathcal{A}(t) \equiv {\rm Tr}\,[\hat{\mu}(t)\hat{\mu}(0)\hat{\rho}_g]$ and $\hat{\rho}_g$ is the ground-state reduced density matrix for the system[73,100]. Fig. 3A presents $\mathcal{A}(t)$ and $\mathcal{A}(\omega)$ for $\Delta_\omega = 0$ at different $\Omega_{\rm R}$ by increasing N, simulated using non-adiabatic partial linearized density matrix (PLDM) dynamics[88]. One sees that $\mathcal{A}(t)$ oscillates with the frequency of $|{\rm G},0\rangle \to |\pm\rangle$ transitions and an overall envelope beating related to $\Omega_{\rm R}$. Increasing $\Omega_{\rm R}$ by increasing N causes $\mathcal{A}(t)$ to oscillate more rapidly and longer, due to the reduction of λ_N (Eq. 12) from the polaron decoupling effect.

On the other hand, with a phenomenological description of the molecular dissipation (c.f. Eq. 1) and under the $N \to \infty$ limit, Ref. 101 derived an analytic expression for the polariton lineshape as follows, $\mathcal{A}(\omega) = \kappa\Gamma N g_{\rm c}^2 / \left|(\omega-\omega_{\rm c}+i\frac{\Gamma}{2\hbar})(\omega-\omega_0+i\frac{\kappa}{2\hbar}) - Ng_{\rm c}^2\right|^2$ (c.f. Eq. 38b of Ref. 101), which is closely connected with the transfer matrix method[102] and in turn gives the polariton linewidth $\Gamma_\pm = -2\,{\rm Im}\,\mathcal{A}(\omega_\pm)$ expressed as follows,

$$\Gamma_- = |X|^2\kappa + |C|^2\Gamma; \quad \Gamma_+ = |C|^2\kappa + |X|^2\Gamma, \tag{15}$$

being the sum of the cavity and exciton broadening weighted by their Hopfield coefficients[44]. However, Eq. 15 do not capture the *subaverage* behavior (*i.e.*, even narrower than Eq. 15) of the polariton linewidth, which is also manifested as non-linear behavior of $\Gamma_\pm$ as a function of $|C|^2$, as observed in experiments[81,82] and in HEOM simulations of the HTC model (Fig. 3B).

For generally detuned cases ($\Delta_\omega \neq 0$), to the best of our knowledge, there is no simple closed-form theoretical expressions for $\Gamma_\pm$. A widely used expression[80–82,103] suggests $\Gamma_- \propto (|C|^4/|X|^2)\Gamma$, emphasizing the nonlinear dependence of the LP linewidth on $|C|^2$, which is recently justified by Rury, *et al.* through an Andersen super-exchange argument[81,82]. By fitting the HEOM simulation with up to $N = 8$ (Fig. 3B), we found that[67]

$$\begin{aligned}\Gamma_- &= |X|^2\kappa + \frac{1}{N}\frac{|C|^4}{|X|^2+|C|^4/N}\Gamma,\\ \Gamma_+ &= |C|^2\kappa + \frac{1}{N}\frac{|X|^4}{|C|^2+|X|^4/N}\Gamma + \hbar k_{+\to {\rm D}},\end{aligned} \tag{16}$$

where the matter component linewidth is narrowed by a factor of $1/N$ due to the polaron decoupling effect for Lorentzian line shape[67]. In Eq. 16, the $\hbar k_{+\to {\rm D}}$ term (see Eq. 13a) accounts for the $|+\rangle \to \{|{\rm D}_k\rangle\}$ relaxation (non-Condon effects)[80,104–106], causing additional broadening of the UP linewidth[81,82]. As shown in Fig. 3B, Eq. 16 (solid lines) accurately captures the non-linear dependence of $\Gamma_\pm$ on $|C|^2$ compared to the HEOM results (open circles), whereas Eq. 15 (dashed lines) disagrees with HEOM.

IV. POLARITON MEDIATED ELECTRON TRANSFER

Recent experiments by Ebbesen and co-workers have shown that the rate of photoisomerization reaction from merocyanine to spiropyran can be suppressed by resonantly coupling the merocyanine to a cavity[3], although the interpretation of such cavity modification is still under debate[107,108]. For the same reaction, Delor and co-workers[36] have shown that the cavity frequency can be tuned to funnel photoexcitations into specific reactant isomers. Kalow, Stern, and co-workers have shown that

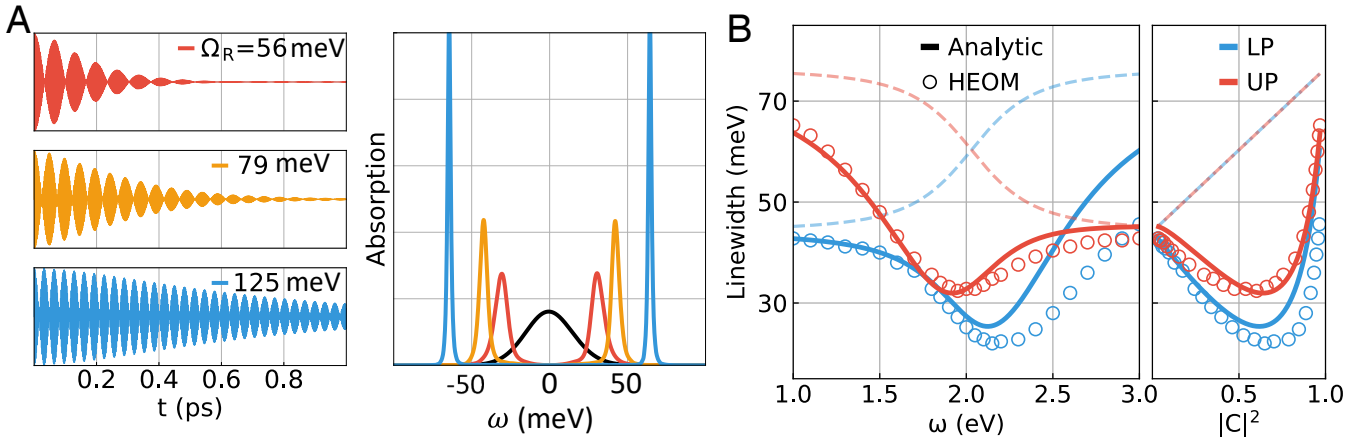

FIG. 3. Polariton spectral functions and linewidth. (**A**) $\mathcal{A}(t)$ (left panel) and $\mathcal{A}(\omega)$ (right panel) with increasing $\hbar\Omega_{\rm R}$ values: 56 meV (red), 79 meV (orange), and 125 meV (blue). The bare molecular absorption (black) is also shown in the right panel. (**B**) Cavity frequency dependence of the polariton linewidths (red for UP and blue for LP). The dashed lines denote the result of Eq. 15. Panel (**A**) was generated using theoretical approaches in Ref. 88. Panel (**B**) was adapted with permission from Ref. 67, copyright @ 2024 AIP Publishing.

collective strong coupling to a resonant cavity can accelerate the photoisomerization of fulgide[35], demonstrating that the enhancement is sensitive to the collective quantity $\Omega_{\rm R}$. A detailed review on the progress of polariton photochemistry can be found in Ref. 5.

Despite these experimental discoveries of cavity-modified photochemistry, conceptual questions remain involving how local modifications of photochemistry emerge under collective strong coupling and the role of dark states. To partially address these conceptual questions, we focus on simple models of a polariton-mediated electron transfer (PMET) reaction, which is one of the simplest photochemical reactions[17,109–112].

A. Model Systems for PMET

The model describes a total of N donor-acceptor state pairs $\{|{\rm D}_n\rangle, |{\rm A}_n\rangle\}$, both of which are molecular excited states. The donor and acceptor states are *locally* coupled $\langle {\rm D}_n|\hat{H}_{\rm S}|{\rm A}_m\rangle = V_{\rm DA}\cdot\delta_{nm}$. The donor state $|{\rm D}_n\rangle$ (not to be confused by the dark states $|{\rm D}_k\rangle$ in Eq. 10) is considered as the bright exciton state (previously denoted as $|{\rm E}_n, 0\rangle$ in Eq. 5). The donor states are photo-excitation states that are collectively coupled to the cavity excitation.

$$\hat{H}_{\rm S} = \sum_{n=1}^{N}\left[\hbar\omega_0\hat{\sigma}_n^+\hat{\sigma}_n^- + V_{\rm DA}\left(|{\rm D}_n\rangle\langle{\rm A}_n| + {\rm h.c}\right)\right] + \hat{H}_{\rm A} + \hbar\omega_{\rm c}(\hat{a}^\dagger\hat{a} + \frac{1}{2}) + \hbar g_{\rm c}\sum_{n=1}^{N}\left(\hat{a}^\dagger\hat{\sigma}_n^- + \hat{a}\hat{\sigma}_n^+\right), \qquad (17)$$

where $\hat{\sigma}_n^+ = |{\rm D}_n\rangle\langle{\rm G}|$ and $\hat{\sigma}_n^- = |{\rm G}\rangle\langle{\rm D}_n|$, with $|{\rm D}_n\rangle$ as the $n_{\rm th}$ molecule's electron donor state, and the acceptor Hamiltonian is $\hat{H}_{\rm A} = \sum_n \hbar\omega_{\rm A}|{\rm A}_n\rangle\langle{\rm A}_n|$ with $|{\rm A}_n\rangle$ as the $n_{\rm th}$ molecule's electron acceptor state. Furthermore, there is one collective solvent DOF (Marcus coordinate) per molecular pair, R_n, which couples to both $|{\rm D}_n\rangle$ and $|{\rm A}_n\rangle$ states through $\hat{H}_{\rm B} + \hat{H}_{\rm SB} = \hat{T}_R + \sum_n \frac{1}{2}m_{\rm s}\omega_{\rm s}^2(\hat{R}_n - R_{\rm D}^0)^2|{\rm D}_n\rangle\langle{\rm D}_n| + \frac{1}{2}m_{\rm s}\omega_{\rm s}^2(\hat{R}_n - R_{\rm A}^0)^2|{\rm A}_n\rangle\langle{\rm A}_n| + \frac{1}{2}m_{\rm s}\omega_{\rm s}^2\hat{R}_n^2|{\rm G}\rangle\langle{\rm G}|$, where $m_{\rm s}$ is the effective solvent mass, $\omega_{\rm s}$ is the effective frequency of the collective solvent DOF, and $R_{\rm D}^0$ and $R_{\rm A}^0$ are the equilibrium positions of the donor and acceptor states, respectively. Each solvent DOF R_n is further coupled to a Markovian dissipative environment. A schematic illustration of the model is provided in Fig. 4A-B.

B. Collective PMET Mechanism

In this model, the UP state is $|+\rangle = \sin\Theta\sum_{n=1}^{N}\frac{1}{\sqrt{N}}|{\rm D}_n, 0\rangle + \cos\Theta|{\rm G}, 1\rangle$ (cf. Eq. 6). The coupling between states $|+\rangle$ and $|{\rm A}_n\rangle$ is $V_{+{\rm A}_n} = \langle +|\hat{H}_{\rm S}|{\rm A}_n, 0\rangle = \frac{1}{\sqrt{N}}\sin\Theta\cdot V_{\rm DA}$. For an FGR rate estimation, $k_{+\to{\rm A}_n} \propto |V_{+{\rm A}_n}|^2 \propto 1/N$. This is often referred to as the $1/N$ "dilution" factor as the influence of the collective polariton state on a given molecule n is diluted by the $1/N$ factor[113]. However, the collective PMET rate between the $|+\rangle$ state and *all* possible acceptor states is $k_{+\to{\rm A}} = \sum_{n=1}^{N} k_{+\to{\rm A}_n}$. Importantly, the pre-factor in $k_{+\to{\rm A}}$ is **independent** of N due to the cancellation of the $1/N$ factor in $|V_{+{\rm A}_n}|^2$ with the sum over N acceptor states[1,110]. Using classical Marcus theory (FGR level of theory), $k_{+\to{\rm A}}$ can be explicitly evaluated in Eq. 18 as follows.

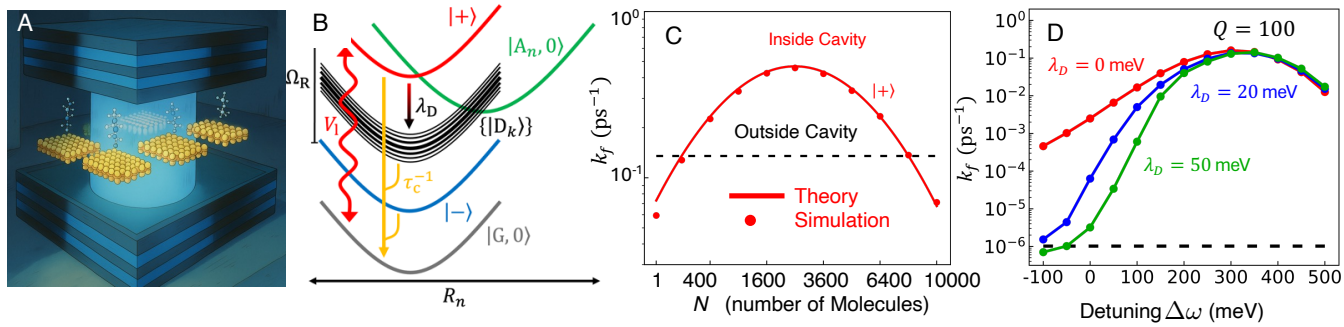

FIG. 4. Model schematics and results for PMET. (**A**) Illustration of several donor-acceptor pairs inside cavity. (**B**) Schematic PESs along molecule n's reaction coordinate R_n with population transfer pathways due to laser pumping (V_l), cavity loss (τ_c^{-1}), and transfer from UP to dark states due to energy disorder induced by λ_D. (**C**) Forward rate constants k_f as a function of N initiated from the $|+\rangle$ state (red) or donor state outside the cavity (black). (**D**) Rate constants as a function of detuning Δ_ω for different donor reorganization energies λ_D initiated from the $|+\rangle$ state. All panels are adapted with permission from Ref. 109.

C. Analytic Theory of the PMET Rate Constant

The collective PMET rate for the process $|+\rangle \rightarrow \{|A_n\rangle\}$ is expressed as

$$k_{+\rightarrow A} = \frac{1}{\hbar}\sin^2\Theta \cdot V_{DA}^2 \sqrt{\frac{\pi}{k_B T \cdot \lambda_A}} \exp\left[-\frac{(\Delta G - \hbar(\Delta_\omega + \Omega_R)/2 + \lambda_A)^2}{4k_B T \cdot \lambda_A}\right], \quad (18)$$

where Ω_R is the Rabi splitting (Eq. 9), and $\Delta_\omega = \omega_c - \omega_0$ is the light-matter detuning (between the cavity and the donor exciton state). The collective quantity Ω_R explicitly appears in the rate constant, through the modification of the effective driving force for the $|+\rangle \rightarrow \{|A_n\rangle\}$ process. As shown in Eq. 18, the only N dependence in $k_{+\rightarrow A}$ comes from the collective Rabi splitting $\Omega_R \propto 2\sqrt{N} g_c$ which changes the ET driving force. This collective N dependence is shown in Fig. 4C where the log of the rate constant $k_{+\rightarrow A}$ has a parabolic dependence on $\sqrt{N}$, with strong agreement between theory and simulation. This rate theory suggests a possible mechanism that depends on the collective coupling Ω_R, even though the light-matter coupling strength per molecule g_c is small. The donor reorganization energy λ_D does not explicitly appear in $k_{+\rightarrow A}$ due to the polaron decoupling effect (Eq. 12). Under the large N limit, the $|+\rangle$ state experiences an effective reorganization energy of $\lambda_D/4N \rightarrow 0$. For arbitrary N, the expression for λ can be found in Eq. 20 of Ref. 109. Nevertheless, λ_D governs the rate of transition from $|+\rangle$ to the dark states manifold (see Eq. 13a, where the coupling strength $c_\alpha^2 \propto \lambda_D$ in $J(\omega)$).

D. Challenges of Cavity Loss

Without external laser pumping of the system, cavity loss (Section II A 3) can inhibit PMET by eliminating the photoexcitation inside the cavity before the excitation can transfer to the acceptor states. To address this challenge, an external CW laser can be tuned to the $|G, 0\rangle \rightarrow |+\rangle$ transition, such that the $|+\rangle$ state population is constantly populated.

This interaction can be described by[18,109] $\hat{H}_l(t) = V_l\left(\hat{a}e^{i\omega_l t} + \hat{a}^\dagger e^{-i\omega_l t}\right)$, with pumping strength V_l and laser frequency $\omega_l = \omega_+$, as described in Ref. 109. This CW laser pumping can replenish lost cavity photons back to the UP state and re-enable PMET to the acceptor states. The simulations of the $k_{+\rightarrow A}$ rate constants in Fig. 4D use a CW laser pumping to replenish $|+\rangle$ state population inside a lossy $\mathcal{Q} = 100$ cavity.

E. Challenges of Decay to Dark States

Disorder in the energies or dipole orientations of molecules coupled to the cavity causes population transfer between bright polariton states and dark states. The PMET model considered here does not contain explicit static energy disorder but experiences thermal-induced energy disorder with an effective donor linewidth of $\sigma = \sqrt{2\lambda_D k_B T}$ due to the donor reorganization energy λ_D. This disorder causes population transfer primarily from the $|+\rangle$ and $|-\rangle$ states to the dark states, which can inhibit PMET enhancement by trapping population in the dark states, which undergo significantly slower ET than the $|+\rangle$ state.

To address this challenge, the transfer rate from the $|+\rangle$ state to the dark states can be significantly reduced by increasing both the Rabi splitting Ω_R and the cavity detuning Δ_ω, as described in Ref. 109. These increases widen the energy gap between the $|+\rangle$ state and the dark states, which can significantly reduce the transfer rate to the dark states due to the phonon bottleneck effect[93], thus allowing for faster PMET from the $|+\rangle$ state. The effect of increasing Δ_ω on the simulated $k_{+\rightarrow A}$ rate constants is shown in Fig. 4D, where larger, positive detun-

ings cause significantly enhanced transfer to the acceptor states compared to resonance ($\Delta_\omega = 0$) for molecules with thermal-induced disorder ($\lambda_{\rm D} > 0$). Additionally, the rate constants for large detunings $\Delta_\omega > 300$ meV become independent of $\lambda_{\rm D}$ due to a large phonon bottleneck effect that diminishes the effect of the dark states.

V. VIBRATIONAL STRONG COUPLING ENABLED POLARITON CHEMISTRY

Vibrational strong coupling (VSC) emerges from the interaction between molecular vibrations and quantized radiation modes in an optical cavity. Recent experiments[37–40,47,114–117] have shown that VSC can modify ground-state chemical reactivity, either by resonantly suppressing or enhancing the reaction rates, offering new strategies in synthetic chemistry. Key features of VSC-modified reactivity include: (1) a resonance effect when the cavity frequency matches that of a molecular vibration[37,40]; (2) maximum effect at normal incidence[37]; (3) enhancement in the *magnitude* of the modification with increasing molecular density (collective effect)[37,38,47]; and (4) changes in reactivity in the absence of optical pumping (thermal activation)[37,39].

A clear mechanistic understanding remains elusive, despite exciting theoretical progress[48,49,118–124]. In particular, all of the existing classic ground-state reaction rate theories fail when used to explain the VSC effects, including the transition state theory (TST), Grote-Hynes theory[121,125], quantum TST[126], Pollak-Grabert-Hänggi theory[122,124], or molecular dynamics simulations (such as Langevin dynamics[127] and ring polymer molecular dynamics[128]), with the conceptual hypothesis that the cavity mode can be viewed and treated as regular nuclear vibrations[121]. Unfortunately, none of them have successfully predicted the correct resonance condition or the sharp resonance peak of the rate constant distribution[121,122,126,127]. Note that the recently developed quantum transition path theory by Limmer, *et al.*[129] can produce a sharp resonance suppresion peak, but does not capture the correct resonance peak position due to anharmonicity of the reaction coordinate. More recent studies[130–134] have emphasized the importance of a full quantum description of the vibrational DOF and/or the photonic DOF, and have shown that strong coupling of a reaction coordinate with a cavity mode boosts the rate constant. An analytic theory to describe this enhancement has been formulated[131,135] and extended to many cavity modes coupling cases to showcase the resonance condition at the normal incidence[135–137].

At the current stage, a clear understanding of the key experimental features (1), (2), and (4) mentioned above has been achieved; nevertheless, experimental feature (3) – the collective effect still remains an important open question. This is because under collective light-matter coupling, these effects observed under the single molecule strong coupling condition usually become minimal due to the large N dilution[48,119,124] and isotropic disorder effects[125]. To address this, we developed a quantum mechanical rate theory for a model ground-state reaction coupled to a cavity mode[125] that captures the above-mentioned basic features of the VSC experiments[137], especially the resonance and the collective behavior of the rate constant modifications.

A. Model System for VSC

We consider a theoretical model where a cavity mode couples to a set of solvent vibrations $\{\mathcal{R}_n\}$ (spectator modes, or rate-promoting vibrations) which in turn couple to a reaction coordinate R_0, as schematically illustrated in Fig. 5A. Instead of the approximated TC-type light-matter interaction Hamiltonian, we use the Pauli-Fierz (PF) Hamiltonian[1] to describe the molecular vibrations collectively coupled to a mode in an optical cavity[125], $\hat{H} = \hat{H}_{\rm S}(\hat{R}_0, \{\hat{\mathcal{R}}_n\}) + \hat{H}_\nu + \hat{H}_{\rm loss}$, where $\hat{H}_{\rm S}$ is the system Hamiltonian that contains the vibrational and photonic DOF, as well as their couplings, $\hat{H}_\nu$ is the dissipative environmental DOF that further couple to R_0 and $\{\mathcal{R}_n\}$, and $\hat{H}_{\rm loss}$ is the cavity loss Hamiltonan, as described in Section II A 3. The system Hamiltonian is expressed as

$$\hat{H}_{\rm S} = \hat{H}_0 + \sum_{n=1}^{N}\left[\frac{1}{2}\hat{\mathcal{P}}_n^2 + \frac{1}{2}\omega_0^2\left(\hat{\mathcal{R}}_n - \frac{\mathcal{C}_n}{\omega_0^2}\hat{R}_0\right)^2\right] + \left[\frac{\hat{p}_{\rm c}^2}{2} + \frac{\omega_{\rm c}^2}{2}\left(\hat{q}_{\rm c} + \sqrt{\frac{2}{\omega_{\rm c}}}\eta_{\rm c}\sum_{n=1}^{N}\hat{\mathcal{R}}_n\right)^2\right] \quad (19)$$

where $\hat{H}_0 = \hat{T}_0 + \hat{V}(\hat{R}_0)$ with $\hat{R}_0$ as the reaction coordinate, $\hat{V}(\hat{R}_0)$ is the ground-state PES (symmetric double-well potential along $\hat{R}_0$). The non-reactive spectator modes $\{\mathcal{R}_n\}$ have identical frequencies ω_0 and are linearly coupled to $\hat{R}_0$ through $\mathcal{C}_n$. This model captures the key features of recent VSC experiments[37,40] and has been employed in previous theoretical studies on VSC-modified reactivities[125,130]. It also reflects the characteristics observed in theoretical simulations of polaritonic vibrational energy relaxation[138], which demonstrate collective and resonance behavior. For example, in Ref. 37, the C-Si is the R_0 reaction coordinate, and Si-(Me)$_3$ is the non-reactive $\mathcal{R}_n$ mode that strongly couple to R_0 (for $N = 1$). In Ref. 40, the spectator mode $\mathcal{R}_n$ could be the N-C-O vibrational mode in the reactant (for $N = 1$). The solvent vibrations could also be viewed as the spectator mode $\{\mathcal{R}_n\}$ (for $N \gg 1$), which was studied in recent VSC theoretical investigations[125,130].

In the last term of Eq. 19, $\hat{q}_{\rm c} = \sqrt{\hbar/(2\omega_{\rm c})}(\hat{a}^\dagger + \hat{a})$ and $\hat{p}_{\rm c} = i\sqrt{\hbar\omega_{\rm c}/2}(\hat{a}^\dagger - \hat{a})$ are the cavity field operators, with $\omega_{\rm c}$ as the cavity frequency and $\eta_{\rm c} = \sqrt{1/(2\hbar\omega_{\rm c}\epsilon_0\mathcal{V})}$ is the light-matter coupling strength. Note that in Eq. 19, we have assumed that the vibrational transition dipole operators are linear[119,121,130] such that $\hat{\boldsymbol{\mu}}(\mathcal{R}_n) \cdot \hat{\mathbf{e}} \approx$

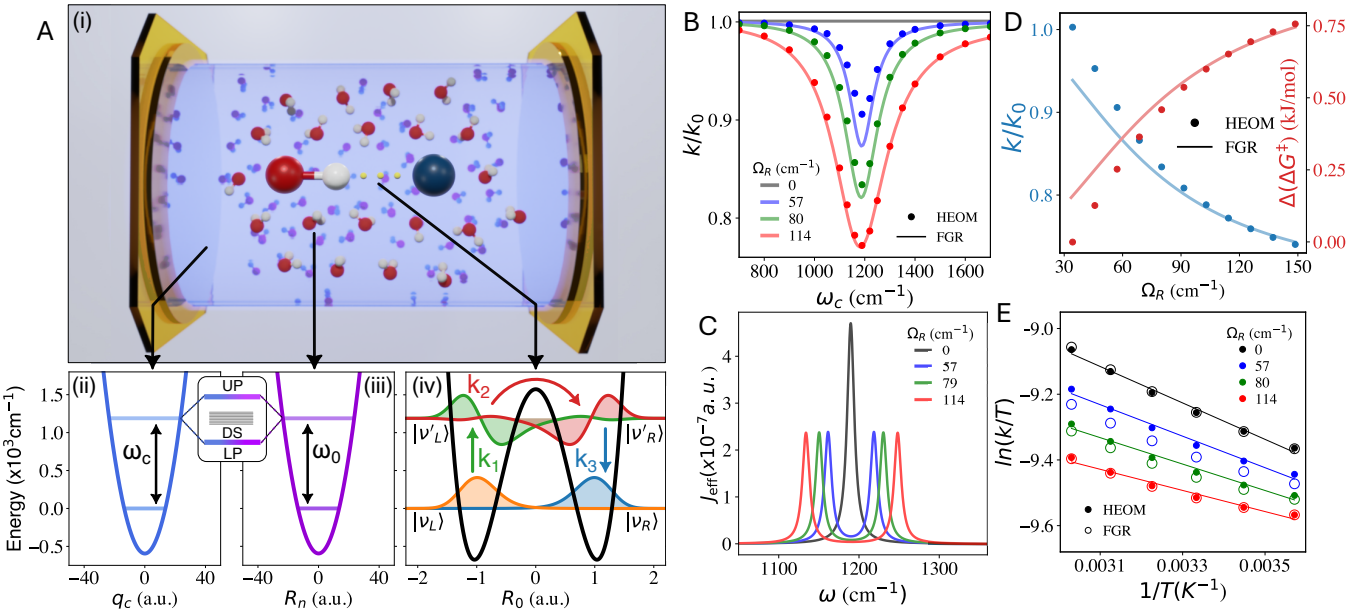

FIG. 5. Model schematics and results for VSC modified ground-state chemistry. (**A**) Schematic illustration of a set of solvent vibrations coupled to the cavity radiation field as well as a reaction coordinate. (**B**) Normalized rate constant profile (with respect to the outside cavity case k_0) as a function of cavity frequency ω_c at different $\hbar\Omega_R$. (**C**) Effective spectral density $J_{\text{eff}}(\omega)$ (Eq. 22) for different $\hbar\Omega_R$ values, where the two peaks correspond to the polariton modes. (**D**) Ratio of the rate constant inside and outside cavity, and effective free energy barrier change $\Delta(\Delta G^{\ddagger})$ at resonance as a function of $\hbar\Omega_R$. (**E**) Eyring plot at various $\hbar\Omega_R$ (at resonance). Note that we have neglected $\hbar$ in all panels that associated with Ω_R. All panels were adapted with permission from Ref. 137.

$\hat{\mathcal{R}}_n \cdot \cos\varphi_n \approx \hat{\mathcal{R}}_n$ (no orientation disorder), where $\hat{\mathbf{e}}$ is the field polarization direction. Under the resonance condition, the overall Rabi splitting[1,46,48] is expressed as $\Omega_R = 2\sqrt{N}\eta_c\omega_c\langle 0|\hat{\mu}(\mathcal{R}_n)|1\rangle \approx 2\sqrt{N}\eta_c\omega_c\langle 0|\hat{\mathcal{R}}_n|1\rangle$ (where $|0\rangle$ and $|1\rangle$ are the ground and first excited states of $\mathcal{R}_n$). The cavity mode couples collectively to all solvent modes $\{\mathcal{R}_n\}$ through η_c. This results in delocalized interactions that can be observed from the Rabi splitting in spectroscopy[139].

B. Reaction Mechanism and Hypothesis

Under a thermal initial condition, the reaction coordinate R_0 undergoes a barrier-crossing process[140,141], where the transition state is reached and finally relaxes to the product configuration. Quantum mechanically, this process is described as

$$|\nu_L\rangle \xrightarrow{k_1} |\nu'_L\rangle \xrightarrow{k_2} |\nu'_R\rangle \xrightarrow{k_3} |\nu_R\rangle, \tag{20}$$

where the system is first thermally excited from the vibrational ground state ($|\nu_L\rangle$) to the excited state ($|\nu'_L\rangle$) of the left side of the well (reactant). This excited state then tunnels to a vibrational excited state ($|\nu'_R\rangle$) on the right side of the well (products), which relaxes to its ground state ($|\nu_R\rangle$), as depicted in Fig. 5A panel (iv). The vibrational frequency $\omega_0 \equiv (E_{\nu'_L} - E_{\nu_L})/\hbar$ of the reactant corresponds to the transition $|\nu_L\rangle \to |\nu'_L\rangle$, and is chosen to match the frequency of $\{\mathcal{R}_n\}$. Exact quantum dynamics simulations suggests that, under the energy-diffusion-limited regime of the reaction (before Kramers turnover[140,141]), the initial vibrational excitation ($|\nu_L\rangle \to |\nu'_L\rangle$) is rate-limiting, with $k_1 \ll k_2, k_3$. This leads to a steady state population of the intermediate states $|\nu'_L\rangle$ and $|\nu'_R\rangle$, and the overall reaction rate is approximately given by $k \approx k_1$. However, when the reaction barrier is low, k_1 is no longer rate-limiting and cavity coupling no longer significantly affects the overall rate. This may explain the absence of VSC effects in low-barrier reactions[142,143].

The $|\nu_L\rangle \to |\nu'_L\rangle$ transition is mainly driven by the energy exchange between reaction coordinate R_0 and the spectator modes $\{\mathcal{R}_n\}$. When these modes are resonantly coupled to the cavity, the light-matter hybrid system has a set of polaritonic modes with frequencies $\omega_\pm = \omega_0 \pm \Omega_R/2$, effectively shifting the energy away from ω_0 and thus suppressing the influence of $\{\mathcal{R}_n\}$ on the $|\nu_L\rangle \to |\nu'_L\rangle$ transition. This suppression can also be understood as a *fast energy exchange* among the strongly coupled $\{\mathcal{R}_n\}$ and $\hat{q}_c$ at the Rabi frequency Ω_R. This energy redistribution effectively decouples $\{\mathcal{R}_n\}$ from the $|\nu_L\rangle \to |\nu'_L\rangle$ transition, reducing the value of k_1. Since this step remains rate-limiting for the reaction process, the influence of the cavity on k_1 manifests in the entire apparent rate constant of the reaction, as $k \approx k_1$.

Based on this mechanism, the impact of VSC on the

rate is solely attributed to the cavity interacting with the spectator modes. This is further confirmed by quantum dynamics simulations (Fig. S2 in Ref. 137), where the steady-state population of the $|\nu_{\rm L}'\rangle$ state is reduced when coupled to the cavity. To quantify the effect of the cavity on the chemical reactivity, we express the ratio of the rate constant inside and outside the cavity as

$$k/k_0 = k_{\rm D}/k_0 + \alpha \cdot k_{\rm VSC}/k_0, \tag{21}$$

where k_0 is the rate constant outside the cavity, $k_{\rm D}$ is the rate constant for the double-well potential without coupling to any spectator modes $\{\mathcal{R}_n\}$ or the cavity mode $q_{\rm c}$, and $k_{\rm VSC}$ is the contribution of the spectator modes to the overall rate with α as a constant scaling parameter. Outside the cavity, the ratio $k_{\rm VSC}/k_0$ peaks when $\{\mathcal{R}_n\}$ modes resonate with the transition $|\nu_{\rm L}\rangle \to |\nu_{\rm L}'\rangle$, enhancing vibration along R_0. Inside the cavity, this ratio lessens with light-matter coupling and eventually reaches zero as the modes no longer affect rate, with $k \sim k_{\rm D}$. This indicates a "polaron decoupling" effect[52,53,67,120], where cavity and spectator mode resonance inhibits energy flow to R_0, enabling analytic rate constant theory based on FGR, consistent with VSC findings.

C. Analytic Theory of $k_{\rm VSC}$ Rate Constant

We use FGR to evaluate the $|\nu_{\rm L}\rangle \to |\nu_{\rm L}'\rangle$ transition rate constant, resulting in

$$k_{\rm VSC} = 2|\Delta|^2 \int_0^\infty d\omega \mathcal{A}_0(\omega-\omega_0) e^{-\beta\hbar\omega_0} \times \frac{\Lambda\omega_0^2 \cdot \omega\Gamma_{\mathcal{R}}(\omega)}{\left[\omega_0^2-\omega^2+\Pi(\omega)\right]^2 + \left[\omega\Gamma_{\mathcal{R}}(\omega)\right]^2}, \tag{22}$$

where ω_0 is the vibrational frequency for $\{\mathcal{R}_n\}$ (with $n \in \{1,\cdots,N\}$) as well as for reaction coordinate R_0, Δ is the transition amplitude for $|\nu_{\rm L}\rangle \to |\nu_{\rm L}'\rangle$ associated with R_0, and $\mathcal{A}_0(\omega-\omega_0)$ accounts for the broadening of this transition due to the local environmental fluctuations. In addition, $\Gamma_{\mathcal{R}}$ characterizes the excitation decay rate in the $\{\mathcal{R}_n\}$ and cavity modes, and $\Pi(\omega)$ characterizes the cavity effect over $\{\mathcal{R}_n\}$. These are expressed as

$$\Gamma_{\mathcal{R}}(\omega) = \frac{2N\eta_{\rm c}^2 \cdot \omega_{\rm c}^3 \tau_{\rm c}^{-1}}{(\omega_{\rm c}^2-\omega^2)^2 + \omega^2\tau_{\rm c}^{-2}} + \frac{2\lambda_{\mathcal{R}}}{\gamma_{\mathcal{R}}},$$
$$\Pi(\omega) = 2N\eta_{\rm c}^2\omega_{\rm c}\omega^2 \cdot \frac{(\omega^2-\omega_{\rm c}^2+\tau_{\rm c}^{-2})}{(\omega_{\rm c}^2-\omega^2)^2 + \omega^2\tau_{\rm c}^{-2}},$$

where $\lambda_{\mathcal{R}}$ and $\gamma_{\mathcal{R}}$ are phonon bath parameters for $\{\mathcal{R}_n\}$ modes with a spectral density $J(\omega) = \frac{2\lambda_{\mathcal{R}}\gamma_{\mathcal{R}}\omega}{\omega^2+\gamma_{\mathcal{R}}^2}$. Interestingly, $k_{\rm VSC}$ contains collective quantities, including the collective Rabi splitting $\Omega_{\rm R}^2 \propto Ng_{\rm c}^2$, as well as the collective solvent reorganization energy $\Lambda = \sum_{n=1}^N \mathcal{C}_n^2/2\omega_0^2$ that accounts for the interactions between $\{\mathcal{R}_n\}$ and R_0.

D. Behavior of the Rate Theory and Connections with Experiments

We briefly discuss the key features of the rate constant theory in Eq. 22 and its connection with experiments.

1. Resonance Suppression

The analytic theory $k_{\rm VSC}$ predicts a sharp resonance suppression of the rate constant. Fig. 5B presents the cavity frequency dependence of k/k_0 with the maximum suppression achieved at $\omega_{\rm c} = \omega_0$. The FGR expression (Eq. 22, solid lines) accurately captures the cavity frequency dependence of the rate constants for a wide range of $\Omega_{\rm R}$, agreeing with HEOM results (dots). This suppression can be interpreted from the effective spectral density $J_{\rm eff}(\omega)$ (see Fig. 5C and Eq. 22) as it accounts for the effective coupling from $\{\mathcal{R}_n\}$ on R_0. Coupling the cavity splits $J_{\rm eff}(\omega)$ into two peaks. The separation between these peaks and the $|\nu_{\rm L}\rangle \to |\nu_{\rm L}'\rangle$ transition is proportional to $\Omega_{\rm R}$, with frequencies that are nearly identical to the vibrational polariton frequencies. Note that the dark modes in this model do not couple to R_0 due to symmetry. As such, $k_{\rm VSC}$ in Eq. 22 quantitatively matches the HEOM results and is capable of describing the sharp resonance behavior observed in the experiments[37,40].

2. Scaling with the collective Rabi splitting

Under the resonance condition $\omega_{\rm c} = \omega_0$, (Eq. 22) predicts that $k_{\rm VSC} \propto 1/\Omega_{\rm R}^2 \propto 1/(N\eta_{\rm c}^2)$. This implies that suppression effects on k/k_0 increase with a $\Omega_{\rm R}^2$ scaling, as presented in the blue curve of Fig. 5D. This trend closely resembles the experimental observations (*e.g.*, Fig. 3D in Ref. 47).

These rate constant changes can be interpreted as the change of the effective free energy barrier $\Delta(\Delta G^\ddagger)$ through[38,47,131] $\Delta(\Delta G^\ddagger) = \Delta G^\ddagger - \Delta G_0^\ddagger = -k_{\rm B}T\ln(k/k_0)$ as presented in Fig. 5D (red). However, this is *not* an actual change in the free-energy barrier, but rather an effective measure of a *purely kinetic* effect. Here, one sees a nonlinear relation of $\Delta(\Delta G^\ddagger)$ with $\Omega_{\rm R}$ that agrees with what has been observed experimentally (e.g. Fig. 3C in Ref. 47). Future experimental investigations should focus on measuring more data points to determine the fundamental scaling relations.

3. Temperature dependence

The temperature dependence of the rate constant is often understood through the Eyring equation[47] based on TST, $\ln(k/T) \propto -\frac{\Delta H^\ddagger}{k_{\rm B}} \cdot \frac{1}{T} + \frac{\Delta S^\ddagger}{k_{\rm B}}$. Fig. 5E presents the temperature dependence of the rate constant outside (black) and inside (color) the cavity. Here, both

the HEOM simulations (full circles) and the FGR theory (open circles) predict the same trend for the changes of $\Delta H^{\ddagger}$ and $\Delta S^{\ddagger}$ as a function of Ω_{R}, which has been experimentally observed[47,144]. We emphasize that based on our current theory, the VSC reaction mechanism is *not* related to the direct modification of $\Delta H^{\ddagger}$ nor $\Delta S^{\ddagger}$ (as proposed by previous theories[121]), but rather how cavity can mediate vibrational excitations; in particular, modifying the rate constant k_1 associated with the $|\nu_{\mathrm{L}}\rangle \to |\nu'_{\mathrm{L}}\rangle$ transition (see Eq. 20). Thus, the changes of the rate constant are purely kinetic.

4. Resonance effect at the normal incidence

According to the photon dispersion in a FP cavity (Eq. 2), there are still a finite number of modes (with $k_{\parallel} \neq 0$), such that $\omega_{\mathbf{k}} = \omega_0$ (oblique incidence), however, despite polaritons being formed under this condition, VSC effects are only observed at $k_{\parallel} = 0$ (normal incidence)[37,48,144].

This normal incidence condition arises from the photonic mode density of states (DOS) inside the cavity, which peaks at $k_{\parallel} \approx 0$[135–137], enhancing the VSC contribution at the normal incidence. The generalization of the k_{VSC} expression to include integration over the photonic DOS indicates that at $k_{\parallel} = 0$, the photonic mode has no in-plane momentum and is spatially confined. This confinement increases the photon's lifetime, leading to the largest magnitude of rate suppression. In contrast, at $k_{\parallel} \neq 0$, the photonic modes have a finite in-plane momentum, reducing its effective lifetime in a given mode volume[136], thus weakening the cavity effects on the system.

E. Limitations and Effect of Disorders

The model we considered above does not consider disorders on the $\{\mathcal{R}_n\} - R_0$ coupling ($\mathcal{C}_n$ in Eq. 19) and the angle between the cavity field polarization and molecular dipole moments (φ_n). In Ref. 137, we explicitly consider these disorders, and the $J_{\mathrm{eff}}(\omega)$ will gradually grow a peak at the $\omega = \omega_0$, which are the vibrational dark states. Increasing the magnitude of disorders (either in $\mathcal{C}_n$ or φ_n in the light-matter coupling term $\hat{\boldsymbol{\mu}}(\mathcal{R}_n)\cdot\hat{\mathbf{e}} \approx \hat{\mathcal{R}}_n \cdot \cos\varphi_n$) leads to the appearance of these dark states in the effective spectral density that couple to R_0, which will influence the rate constant in the same way as outside the cavity. As a result, cavity effects can only persist under moderate disorders (see Fig. 5 in Ref. 137), but diminish under an isotropic distribution of φ_n or a broad variation in $\mathcal{C}_n$.

VI. CONCLUSIONS AND PERSPECTIVE

In this review, we highlighted the necessary theoretical ingredients for describing collective light-matter coupling for many molecules and optical cavity modes. The collective effects are exhibited in more ways than one for various polaritonic systems. For example, the reduced reorganization energy due to the polaron decoupling effect, the modification of the ET driving force, and the effective spectral density in VSC. Furthermore, a number of open questions and controversies in this field have been addressed – including those mentioned in the Introduction. We begun with the HTC Hamiltonian that describes collective light-matter coupling and introduced the concept of polariton and dark states. For polariton photophysics, we discussed the well-understood polariton relaxation dynamics, the decoherence process, and spectral properties – the motional narrowing effect in particular. These polariton photophysical properties are closely related to the polaron decoupling effect. For polariton photochemistry, we considered a model for the PMET reaction, where the collective quantity Ω_{R} explicitly appears in the rate constant expression (to modify the ET driving force). For VSC, we considered a model in which the solvent (spectator vibrations) is collectively coupled to the cavity mode, as well as a reaction coordinate, where both Ω_{R} and solvent reorganization energy Λ (also a collective quantity) show up in the rate constant modification. These theoretical investigations shed light on how collective light-matter coupling could influence polariton dynamics, coherence, spectroscopy, photochemical reactions, and VSC chemistry. Future investigations should focus on exploring the validity of the proposed mechanisms with experimental measurements along with testing the scaling relations predicted by the analytic expressions (*e.g.*, Eq. 18 and Eq. 22). Ultimately, the collective strong coupling regime represents not merely a perturbation to matter, but a fundamentally new avenue for controlling quantum states and designing hybrid light-matter systems. As our understanding deepens, it holds the promise to redefine paradigms in chemistry, physics, and materials science alike.

DISCLOSURE STATEMENT

The authors are not aware of any affiliations, memberships, funding, or financial holdings that might be perceived as affecting the objectivity of this review.

ACKNOWLEDGMENTS

This work was supported by the Air Force Office of Scientific Research under AFOSR Award No. FA9550-23-1-0438. W.Y. appreciates the support of the Moses Passer Graduate Fellowship from the University of Rochester (U of R). S.M.V. appreciates the support of the Esther

M. Conwell Graduate Fellowship and the Elon Huntington Hooker Fellowship from U of R. M.E.M. appreciates the support of the Wu Fellowship and the Messersmith Dissertation Fellowship from U of R. P.H. appreciates the support of the Cottrell Scholar Award (a program by the Research Corporation for Science Advancement). We appreciate the valuable contributions of the polariton coherence simulations from Ben Chng, the development of non-equilibrium rate theory from Yifan Lai, as well as the collective PMET and VSC mechanism from Arkajit Mandal. W.Y. thanks valuable comments from Xuecheng Tao. We appreciate valuable discussions with Milan Delor, Andrew Musser, Tal Schwartz, Minjung Son, Aaron Rury, Steve Cundiff, Nick Vamivakas, and Todd Krauss.

[1] A. Mandal, M. A. Taylor, B. M. Weight, E. R. Koessler, X. Li, and P. Huo, "Theoretical advances in polariton chemistry and molecular cavity quantum electrodynamics," Chem. Rev. **123**, 9786–9879 (2023).

[2] T. Schwartz, J. A. Hutchison, C. Genet, and T. W. Ebbesen, "Reversible switching of ultrastrong light-molecule coupling," Phys. Rev. Lett. **106**, 196405 (2011).

[3] J. A. Hutchison, T. Schwartz, C. Genet, E. Devaux, and T. W. Ebbesen, "Modifying Chemical Landscapes by Coupling to Vacuum Fields," Angew. Chem. Int. Ed. **51**, 1592–1596 (2012).

[4] T. W. Ebbesen, "Hybrid light–matter states in a molecular and material science perspective," Acc. Chem. Res. **49**, 2403–2412 (2016).

[5] R. Bhuyan, J. Mony, O. Kotov, G. W. Castellanos, J. G. Rivas, T. O. Shegai, and K. Börjesson, "The Rise and Current Status of Polaritonic Photochemistry and Photophysics," Chem. Rev. **123**, 10877–10919 (2023).

[6] B. Xiang, R. F. Ribeiro, M. Du, L. Chen, Z. Yang, J. Wang, J. Yuen-Zhou, and W. Xiong, "Intermolecular vibrational energy transfer enabled by microcavity strong light–matter coupling," Science **368**, 665–667 (2020).

[7] T.-T. Chen, M. Du, Z. Yang, J. Yuen-Zhou, and W. Xiong, "Cavity-enabled enhancement of ultrafast intramolecular vibrational redistribution over pseudorotation," Science **378**, 790–794 (2022).

[8] W. Xiong, "Molecular Vibrational Polariton Dynamics: What Can Polaritons Do?" Acc. Chem. Res. **56**, 776–786 (2023).

[9] B. Xiang and W. Xiong, "Molecular Polaritons for Chemistry, Photonics and Quantum Technologies," Chem. Rev. **124**, 2512–2552 (2024).

[10] O. Hirschmann, H. H. Bhakta, and W. Xiong, "The role of IR inactive mode in W(CO)6 polariton relaxation process," Nanophotonics **13**, 2029–2034 (2024).

[11] A. Semenov and A. Nitzan, "Electron transfer in confined electromagnetic fields," J. Chem. Phys. **150**, 174122 (2019).

[12] S. N. Chowdhury, A. Mandal, and P. Huo, "Ring polymer quantization of the photon field in polariton chemistry," J. Chem. Phys. **154**, 044109 (2021).

[13] M. A. C. Saller, Y. Lai, and E. Geva, "An Accurate Linearized Semiclassical Approach for Calculating Cavity-Modified Charge Transfer Rate Constants," J. Phys. Chem. Lett. **13**, 2330–2337 (2022).

[14] M. A. C. Saller, Y. Lai, and E. Geva, "Cavity-modified Fermi's golden rule rate constants: Beyond the single mode approximation," J. Chem. Phys. **159**, 151105 (2023).

[15] M. A. C. Saller, Y. Lai, and E. Geva, "Cavity-Modified Fermi's Golden Rule Rate Constants from Cavity-Free Inputs," J. Phys. Chem. C **127**, 3154–3164 (2023).

[16] S. K. Sharma and H.-T. Chen, "Unraveling abnormal collective effects via the non-monotonic number dependence of electron transfer in confined electromagnetic fields," J. Chem. Phys. **161**, 104102 (2024).

[17] A. Mandal, T. D. Krauss, and P. Huo, "Polariton-Mediated Electron Transfer via Cavity Quantum Electrodynamics," J. Phys. Chem. B **124**, 6321–6340 (2020).

[18] L. Qiu, A. Mandal, O. Morshed, M. T. Meidenbauer, W. Girten, P. Huo, A. N. Vamivakas, and T. D. Krauss, "Molecular Polaritons Generated from Strong Coupling between CdSe Nanoplatelets and a Dielectric Optical Cavity," J. Phys. Chem. Lett. **12**, 5030–5038 (2021).

[19] K. Peng and E. Rabani, "Polaritonic Bottleneck in Colloidal Quantum Dots," Nano Lett. **23**, 10587–10593 (2023).

[20] O. Morshed, M. Amin, N. M. B. Cogan, E. R. Koessler, R. Collison, T. M. Tumiel, W. Girten, F. Awan, L. Mathis, P. Huo, A. N. Vamivakas, T. W. Odom, and T. D. Krauss, "Room-temperature strong coupling between CdSe nanoplatelets and a metal–DBR Fabry–Pérot cavity," J. Chem. Phys. **161**, 014710 (2024).

[21] M. Amin, E. R. Koessler, O. Morshed, F. Awan, N. M. B. Cogan, R. Collison, T. M. Tumiel, W. Girten, C. Leiter, A. N. Vamivakas, P. Huo, and T. D. Krauss, "Cavity Controlled Upconversion in CdSe Nanoplatelet Polaritons," ACS Nano **18**, 21388–21398 (2024).

[22] S. Hou, M. Khatoniar, K. Ding, Y. Qu, A. Napolov, V. M. Menon, and S. R. Forrest, "Ultralong-Range Energy Transport in a Disordered Organic Semiconductor at Room Temperature Via Coherent Exciton-Polariton Propagation," Adv. Mater. **32**, 2002127 (2020).

[23] R. Pandya, R. Y. S. Chen, Q. Gu, J. Sung, C. Schnedermann, O. S. Ojambati, R. Chikkaraddy, J. Gorman, G. Jacucci, O. D. Onelli, T. Willhammar, D. N. Johnstone, S. M. Collins, P. A. Midgley, F. Auras, T. Baikie, R. Jayaprakash, F. Mathevet, R. Soucek, M. Du, A. M. Alvertis, A. Ashoka, S. Vignolini, D. G. Lidzey, J. J. Baumberg, R. H. Friend, T. Barisien, L. Legrand, A. W. Chin, J. Yuen-Zhou, S. K. Saikin, P. Kukura, A. J. Musser, and A. Rao, "Microcavity-like exciton-polaritons can be the primary photoexcitation in bare organic semiconductors," Nat. Commun. **12**, 6519 (2021).

[24] R. Pandya, A. Ashoka, K. Georgiou, J. Sung, R. Jayaprakash, S. Renken, L. Gai, Z. Shen, A. Rao, and A. J. Musser, "Tuning the Coherent Propagation of Organic Exciton-Polaritons through Dark State Delocalization," Adv. Sci. **9**, 2105569 (2022).

[25] D. Xu, A. Mandal, J. M. Baxter, S. W. Cheng, I. Lee, H. Su, S. Liu, D. R. Reichman, and M. Delor, "Ultrafast imaging of polariton propagation and interactions," Nat. Commun. **14**, 3881 (2023).

[26] S. W. Cheng, D. Xu, H. Su, J. M. Baxter, L. N. Holtzman, K. Watanabe, T. Taniguchi, J. C. Hone, K. Barmak, and M. Delor, "Optical Imaging of Ultrafast Phonon-Polariton Propagation through an Excitonic Sensor," Nano Lett. **23**, 9936–9942 (2023).

[27] M. Balasubrahmaniyam, A. Simkhovich, A. Golombek, G. Sandik, G. Ankonina, and T. Schwartz, "From enhanced diffusion to ultrafast ballistic motion of hybrid light–matter excitations," Nat. Mater. **22**, 338–344 (2023).

[28] G. Sandik, J. Feist, F. J. García-Vidal, and T. Schwartz, "Cavity-enhanced energy transport in molecular systems," Nat. Mater. **null**, null (2024).

[29] W. Ying, B. X. Chng, M. Delor, and P. Huo, "Microscopic theory of polariton group velocity renormalization," Nat. Commun. **16**, 6950 (2025).

[30] J. Cao, "Generalized Resonance Energy Transfer Theory: Applications to Vibrational Energy Flow in Optical Cavities," J. Phys. Chem. Lett. **13**, 10943–10951 (2022).

[31] I. Sokolovskii, R. H. Tichauer, D. Morozov, J. Feist, and G. Groenhof, "Multi-scale molecular dynamics simulations of enhanced energy transfer in organic molecules under strong coupling," Nat. Commun. **14**, 6613 (2023).

[32] K. Peng and E. Rabani, "Polariton-assisted incoherent to coherent excitation energy transfer between colloidal nanocrystal quantum dots," J. Chem. Phys. **161**, 154107 (2024).

[33]D. G. Angelakis, ed., *Quantum Simulations with Photons and Polaritons: Merging Quantum Optics with Condensed Matter Physics* (Springer Cham, 2017).
[34]S. Ghosh and T. C. Liew, "Quantum computing with exciton-polariton condensates," npj Quantum Inf. **6**, 16 (2020).
[35]H. Zeng, J. B. Pérez-Sánchez, C. T. Eckdahl, P. Liu, W. J. Chang, E. A. Weiss, J. A. Kalow, J. Yuen-Zhou, and N. P. Stern, "Control of photoswitching kinetics with strong light–matter coupling in a cavity," J. Am. Chem. Soc. **145**, 19655–19661 (2023).
[36]I. Lee, S. R. Melton, D. Xu, and M. Delor, "Controlling Molecular Photoisomerization in Photonic Cavities through Polariton Funneling," J. Am. Chem. Soc. **146**, 95449553 (2024).
[37]A. Thomas, J. George, A. Shalabney, M. Dryzhakov, S. J. Varma, J. Moran, T. Chervy, X. Zhong, E. Devaux, C. Genet, J. A. Hutchison, and T. W. Ebbesen, "Ground-State Chemical Reactivity under Vibrational Coupling to the Vacuum Electromagnetic Field," Angew. Chem. Int. Ed. **55**, 11462–11466 (2016).
[38]J. Lather, P. Bhatt, A. Thomas, T. W. Ebbesen, and J. George, "Cavity Catalysis by Cooperative Vibrational Strong Coupling of Reactant and Solvent Molecules," Angew. Chem. Int. Ed. **58**, 10635–10638 (2019).
[39]A. Thomas and L. Lethuillier-Karl and K. Nagarajan and R. M. A. Vergauwe and J. George and T. Chervy and A. Shalabney and E. Devaux and C. Genet and J. Moran and T. W. Ebbesen, "Tilting a ground-state reactivity landscape by vibrational strong coupling," Science **363**, 615–619 (2019).
[40]W. Ahn, J. F. Triana, F. Recabal, F. Herrera, and B. S. Simpkins, "Modification of ground-state chemical reactivity via light–matter coherence in infrared cavities," Science **380**, 1165–1168 (2023).
[41]K. Müller, K. A. Fischer, A. Rundquist, C. Dory, K. G. Lagoudakis, T. Sarmiento, Y. A. Kelaita, V. Borish, and J. Vučković, "Ultrafast polariton-phonon dynamics of strongly coupled quantum dot-nanocavity systems," Phys. Rev. X **5**, 031006 (2015).
[42]F. P. Laussy, E. del Valle, M. Schrapp, A. Laucht, and J. J. Finley, "Climbing the Jaynes–Cummings ladder by photon counting," J. Nanophotonics **6**, 061803–061803 (2012).
[43]S. Mukamel, A. Li, and M. Galperin, "Exceptional points treatment of cavity spectroscopies," J. Chem. Phys. **158**, 154106 (2023).
[44]H. Deng, H. Haug, and Y. Yamamoto, "Exciton-polariton Bose-Einstein condensation," Rev. Mod. Phys. **82**, 1489–1537 (2010).
[45]K. Schwennicke, A. Koner, J. B. Perez-Sanchez, W. Xiong, N. C. Giebink, M. L. Weichman, and J. Yuen-Zhou, "Unlocking delocalization: how much coupling strength is required to overcome energy disorder in molecular polaritons?" Chem. Sci. **16**, 4676 (2025).
[46]J. del Pino, J. Feist, and F. J. Garcia-Vidal, "Quantum theory of collective strong coupling of molecular vibrations with a microcavity mode," New J. Phys. **17**, 053040 (2015).
[47]A. Thomas, A. Jayachandran, L. Lethuillier-Karl, R. M. Vergauwe, K. Nagarajan, E. Devaux, C. Genet, J. Moran, and T. W. Ebbesen, "Ground state chemistry under vibrational strong coupling: dependence of thermodynamic parameters on the Rabi splitting energy," Nanophotonics **9**, 249–255 (2020).
[48]J. A. Campos-Gonzalez-Angulo, Y. R. Poh, M. Du, and J. Yuen-Zhou, "Swinging between shine and shadow: Theoretical advances on thermally activated vibropolaritonic chemistry," J. Chem. Phys. **158**, 230901 (2023).
[49]B. S. Simpkins, A. D. Dunkelberger, and I. Vurgaftman, "Control, Modulation, and Analytical Descriptions of Vibrational Strong Coupling," Chem. Rev. **123**, 5020–5048 (2023).
[50]M. Tavis and F. W. Cummings, "Exact Solution for an N-Molecule—Radiation-Field Hamiltonian," Phys. Rev. **170**, 379–384 (1968).
[51]M. Tavis and F. W. Cummings, "Approximate Solutions for an N-Molecule-Radiation-Field Hamiltonian," Phys. Rev. **188**, 692–695 (1969).
[52]F. Herrera and F. C. Spano, "Cavity-Controlled Chemistry in Molecular Ensembles," Phys. Rev. Lett. **116**, 238301 (2016).
[53]F. Herrera and F. C. Spano, "Theory of nanoscale organic cavities: The essential role of vibration-photon dressed states," ACS Photonics **5**, 65–79 (2018).
[54]M. A. Zeb, P. G. Kirton, and J. Keeling, "Exact states and spectra of vibrationally dressed polaritons," ACS Photonics **5**, 249–257 (2018).
[55]F. Herrera and F. C. Spano, "Absorption and photoluminescence in organic cavity QED," Phys. Rev. A **95**, 053867 (2017).
[56]K. B. Arnardottir, A. J. Moilanen, A. Strashko, P. Törmä, and J. Keeling, "Multimode Organic Polariton Lasing," Phys. Rev. Lett. **125**, 233603 (2020).
[57]J. Keeling and S. Kéna-Cohen, "Bose–Einstein Condensation of Exciton-Polaritons in Organic Microcavities," Annu. Rev. Phys. Chem. **71**, 435–459 (2020).
[58]A. Caldeira and A. Leggett, "Quantum tunnelling in a dissipative system," Ann. Phys. **149**, 374–456 (1983).
[59]M. K. Lee, P. Huo, and D. F. Coker, "Semiclassical path integral dynamics: Photosynthetic energy transfer with realistic environment interactions," Annu. Rev. Phys. Chem. **67**, 639–668 (2016).
[60]S. Dutra and G. Nienhuis, "Quantized mode of a leaky cavity," Phys. Rev. A **62**, 063805 (2000).
[61]S. Dutra and G. Nienhuis, "Derivation of a Hamiltonian for photon decay in acavity," J. Opt. B: Quantum Semiclass. Opt. **2**, 584 (2000).
[62]S. M. Dutra, *Cavity quantum electrodynamics: the strange theory of light in a box* (John Wiley & Sons, 2005).
[63]E. R. Koessler, A. Mandal, and P. Huo, "Incorporating Lindblad decay dynamics into mixed quantum-classical simulations," J. Chem. Phys. **157**, 064101 (2022).
[64]J. Hopfield, "Theory of the contribution of excitons to the complex dielectric constant of crystals," Phys. Rev. **112**, 1555 (1958).
[65]T. E. Li, A. Nitzan, and J. E. Subotnik, "Polariton relaxation under vibrational strong coupling: Comparing cavity molecular dynamics simulations against Fermi's golden rule rate," J. Chem. Phys. **156**, 134106 (2022).
[66]Y. Lai, W. Ying, and P. Huo, "Non-equilibrium rate theory for polariton relaxation dynamics," J. Chem. Phys. **161**, 104109 (2024).
[67]W. Ying, M. E. Mondal, and P. Huo, "Theory and quantum dynamics simulations of exciton-polariton motional narrowing," J. Chem. Phys. **161**, 064105 (2024).
[68]A. Mandal, S. Montillo Vega, and P. Huo, "Polarized Fock States and the Dynamical Casimir Effect in Molecular Cavity Quantum Electrodynamics," J. Phys. Chem. Lett. **11**, 9215–9223 (2020).
[69]W. Zhou, D. Hu, A. Mandal, and P. Huo, "Nuclear gradient expressions for molecular cavity quantum electrodynamics simulations using mixed quantum-classical methods," J. Chem. Phys. **157**, 104118 (2022).
[70]D. Hu, A. Mandal, B. M. Weight, and P. Huo, "Quasi-diabatic propagation scheme for simulating polariton chemistry," J. Chem. Phys. **157**, 194109 (2022).
[71]D. Hu and P. Huo, "Ab Initio Molecular Cavity Quantum Electrodynamics Simulations Using Machine Learning Models," J. Chem. Theory Comput. **19**, 2353–2368 (2023).
[72]S. Takahashi and K. Watanabe, "Decoupling from a Thermal Bath via Molecular Polariton Formation," J. Phys. Chem. Lett. **11**, 1349–1356 (2020).
[73]A. Nitzan, *Chemical Dynamics in Condensed Phases: Relaxation, Transfer and Reactions in Condensed Molecular Systems*, Oxford Graduate Texts (Oxford, New York, 2006).
[74]T. Schwartz, J. A. Hutchison, J. Léonard, C. Genet, S. Haacke, and T. W. Ebbesen, "Polariton Dynamics under Strong Light–Molecule Coupling," ChemPhysChem **14**, 125–131 (2013).

[75] A. Canaguier-Durand, C. Genet, A. Lambrecht, T. W. Ebbesen, and S. Reynaud, "Non-Markovian polariton dynamics in organic strong coupling," Eur. Phys. J. D **69**, 24 (2015).
[76] J. Mony, M. Hertzog, K. Kushwaha, and K. Börjesson, "Angle-Independent Polariton Emission Lifetime Shown by Perylene Hybridized to the Vacuum Field Inside a Fabry–Pérot Cavity," J. Phys. Chem. C **122**, 24917–24923 (2018).
[77] B. Xiang, R. F. Ribeiro, L. Chen, J. Wang, M. Du, J. Yuen-Zhou, and W. Xiong, "State-Selective Polariton to Dark State Relaxation Dynamics," J. Phys. Chem. A **123**, 5918–5927 (2019).
[78] A. G. Avramenko and A. S. Rury, "Quantum Control of Ultrafast Internal Conversion Using Nanoconfined Virtual Photons," J. Phys. Chem. Lett. **11**, 1013–1021 (2020).
[79] M. Laitz, A. E. K. Kaplan, J. Deschamps, U. Barotov, A. H. Proppe, I. García-Benito, A. Osherov, G. Grancini, D. W. deQuilettes, K. A. Nelson, M. G. Bawendi, and V. Bulović, "Uncovering temperature-dependent exciton-polariton relaxation mechanisms in hybrid organic-inorganic perovskites," Nat. Commun. **14**, 2426 (2023).
[80] D. M. Whittaker, P. Kinsler, T. A. Fisher, M. S. Skolnick, A. Armitage, A. M. Afshar, M. D. Sturge, and J. S. Roberts, "Motional Narrowing in Semiconductor Microcavities," Phys. Rev. Lett. **77**, 4792–4795 (1996).
[81] S. T. Wanasinghe, A. Gjoni, W. Burson, C. Majeski, B. Zaslona, and A. S. Rury, "Motional Narrowing through Photonic Exchange: Rational Suppression of Excitonic Disorder from Molecular Cavity Polariton Formation," J. Phys. Chem. Lett. **15**, 2405–2418 (2024).
[82] E. O. Odewale, S. T. Wanasinghe, and A. S. Rury, "Assessing the Determinants of Cavity Polariton Relaxation Using Angle-Resolved Photoluminescence Excitation Spectroscopy," J. Phys. Chem. Lett. **15**, 5705–5713 (2024).
[83] J. del Pino, F. A. Y. N. Schröder, A. W. Chin, J. Feist, and F. J. Garcia-Vidal, "Tensor Network Simulation of Non-Markovian Dynamics in Organic Polaritons," Phys. Rev. Lett. **121**, 227401 (2018).
[84] J. del Pino, F. A. Y. N. Schröder, A. W. Chin, J. Feist, and F. J. Garcia-Vidal, "Tensor network simulation of polaron-polaritons in organic microcavities," Phys. Rev. B **98**, 165416 (2018).
[85] K. Sun, C. Dou, M. F. Gelin, and Y. Zhao, "Dynamics of disordered Tavis–Cummings and Holstein–Tavis–Cummings models," J. Chem. Phys. **156**, 024102 (2022).
[86] E. Hou, K. Sun, M. F. Gelin, and Y. Zhao, "Finite temperature dynamics of the Holstein–Tavis–Cummings model," J. Chem. Phys. **160**, 084116 (2024).
[87] D. Hu, B. X. K. Chng, W. Ying, and P. Huo, "Trajectory-based non-adiabatic simulations of the polariton relaxation dynamics," J. Chem. Phys. **162**, 124113 (2025).
[88] M. E. Mondal, A. N. Vamivakas, S. T. Cundiff, T. D. Krauss, and P. Huo, "Polariton spectra under the collective coupling regime. I. Efficient simulation of linear spectra and quantum dynamics," J. Chem. Phys. **162**, 014114 (2025).
[89] P. Fowler-Wright, B. W. Lovett, and J. Keeling, "Efficient Many-Body Non-Markovian Dynamics of Organic Polaritons," Phys. Rev. Lett. **129**, 173001 (2022).
[90] L. P. Lindoy, A. Mandal, and D. R. Reichman, "Investigating the collective nature of cavity-modified chemical kinetics under vibrational strong coupling," Nanophotonics **13**, 2617–2633 (2024).
[91] J. B. Pérez-Sánchez, A. Koner, N. P. Stern, and J. Yuen-Zhou, "Simulating molecular polaritons in the collective regime using few-molecule models," Proc. Natl. Acad. Sci. U.S.A. **120**, e2219223120 (2023).
[92] J. B. Pérez-Sánchez, A. Koner, S. Raghavan-Chitra, and J. Yuen-Zhou, "CUT-E as a 1/N expansion for multiscale molecular polariton dynamics," J. Chem. Phys. **162**, 064101 (2025).
[93] B. X. K. Chng, W. Ying, Y. Lai, A. N. Vamivakas, S. T. Cundiff, T. D. Krauss, and P. Huo, "Mechanism of Molecular Polariton Decoherence in the Collective Light–Matter Couplings Regime," J. Phys. Chem. Lett. **15**, 11773–11783 (2024).
[94] G. D. Scholes, C. A. DelPo, and B. Kudisch, "Entropy Reorders Polariton States," J. Phys. Chem. Lett. **11**, 6389–6395 (2020).
[95] N. Wu, J. Feist, and F. J. Garcia-Vidal, "When polarons meet polaritons: Exciton-vibration interactions in organic molecules strongly coupled to confined light fields," Phys. Rev. B **94**, 195409 (2016).
[96] G. D. Scholes, "Polaritons and excitons: Hamiltonian design for enhanced coherence," Proc. Math. Phys. Eng. Sci. **476**, 20200278 (2020).
[97] M. E. Mondal, E. R. Koessler, J. Provazza, A. N. Vamivakas, S. T. Cundiff, T. D. Krauss, and P. Huo, "Quantum dynamics simulations of the 2D spectroscopy for exciton polaritons," J. Chem. Phys. **159**, 094102 (2023).
[98] M. E. Mondal, A. N. Vamivakas, S. T. Cundiff, T. D. Krauss, and P. Huo, "Polariton spectra under the collective coupling regime. II. 2D non-linear spectra," J. Chem. Phys. **162**, 074110 (2025).
[99] D. Timmer, M. Gittinger, T. Quenzel, S. Stephan, Y. Zhang, M. F. Schumacher, A. Lützen, M. Silies, S. Tretiak, J.-H. Zhong, *et al.*, "Plasmon mediated coherent population oscillations in molecular aggregates," Nat. Commun. **14**, 8035 (2023).
[100] S. Mukamel, *Principles of Nonlinear Optical Spectroscopy* (Oxford University Press, 1995).
[101] J. Yuen-Zhou and A. Koner, "Linear response of molecular polaritons," J. Chem. Phys. **160**, 154107 (2024).
[102] K. Schwennicke, A. Koner, J. B. Perez-Sanchez, W. Xiong, N. C. Giebink, M. L. Weichman, and J. Yuen-Zhou, "When do molecular polaritons behave like optical filters?" Chem. Soc. Rev. **10.1039/d4cs01024h** (2025).
[103] M. Litinskaia and I. Kaganova, "Motional narrowing in a microcavity: contribution to the lower polariton linewidth," Phys. Lett. A **275**, 292–298 (2000).
[104] V. Savona, C. Piermarocchi, A. Quattropani, F. Tassone, and P. Schwendimann, "Microscopic Theory of Motional Narrowing of Microcavity Polaritons in a Disordered Potential," Phys. Rev. Lett. **78**, 4470–4473 (1997).
[105] D. M. Whittaker, "What Determines Inhomogeneous Linewidths in Semiconductor Microcavities?" Phys. Rev. Lett. **80**, 4791–4794 (1998).
[106] T. Neuman and J. Aizpurua, "Origin of the asymmetric light emission from molecular exciton–polaritons," Optica **5**, 1247 (2018).
[107] P. A. Thomas, W. J. Tan, V. G. Kravets, A. N. Grigorenko, and W. L. Barnes, "Non-Polaritonic Effects in Cavity-Modified Photochemistry," Adv. Mater. **36**, 2309393 (2024).
[108] T. Schwartz and J. A. Hutchison, "On the importance of experimental details: A Comment on "Non-Polaritonic Effects in Cavity-Modified Photochemistry"," arXiv:2403.06001 (2024).
[109] E. R. Koessler, A. Mandal, A. J. Musser, T. D. Krauss, and P. Huo, "Polariton mediated electron transfer under the collective molecule–cavity coupling regime," Chem. Sci. **16**, 11644–11658 (2025).
[110] L. Mauro, K. Caicedo, G. Jonusauskas, and R. Avriller, "Charge-transfer chemical reactions in nanofluidic Fabry-Pérot cavities," Phys. Rev. B **103**, 165412 (2021).
[111] N. T. Phuc, "Super-reaction: The collective enhancement of a reaction rate by molecular polaritons in the presence of energy fluctuations," J. Chem. Phys. **155**, 014308 (2021).
[112] S. K. Sharma and H.-T. Chen, "Unraveling abnormal collective effects via the non-monotonic number dependence of electron transfer in confined electromagnetic fields," J. Chem. Phys. **161**, 104102 (2024).
[113] E. Eizner, L. A. Martínez-Martínez, J. Yuen-Zhou, and S. Kéna-Cohen, "Inverting singlet and triplet excited states using strong light-matter coupling," Sci. Adv. **5**, eaax4482 (2019).
[114] A. Sau, K. Nagarajan, B. Patrahau, L. Lethuillier-Karl, R. M. A. Vergauwe, A. Thomas, J. Moran, C. Genet, and T. W. Ebbesen, "Modifying Woodward–Hoffmann Stereoselectivity Under Vibrational Strong Coupling," Angew. Chem. Int.

Ed. **60**, 5712–5717 (2021).
[115]J. Lather, A. N. K. Thabassum, J. Singh, and J. George, "Cavity catalysis: modifying linear free-energy relationship under cooperative vibrational strong coupling," Chem. Sci. **13**, 195–202 (2022).
[116]K. Hirai, R. Takeda, J. A. Hutchison, and H. Uji-i, "Modulation of Prins Cyclization by Vibrational Strong Coupling," Angew. Chem. Int. Ed. **59**, 5332–5335 (2020).
[117]F. Verdelli, Y.-C. Wei, K. Joseph, M. S. Abdelkhalik, M. Goudarzi, S. H. C. Askes, A. Baldi, E. W. Meijer, and J. Gomez Rivas, "Polaritonic Chemistry Enabled by Non-Local Metasurfaces," Angew. Chem. Int. Ed. **63**, e202409528 (2024).
[118]T. E. Li, A. Nitzan, and J. E. Subotnik, "On the origin of ground-state vacuum-field catalysis: Equilibrium consideration," J. Chem. Phys. **152**, 234107 (2020).
[119]J. A. Campos-Gonzalez-Angulo and J. Yuen-Zhou, "Polaritonic normal modes in transition state theory," J. Chem. Phys. **152**, 161101 (2020).
[120]C. Schäfer, J. Flick, E. Ronca, P. Narang, and A. Rubio, "Shining Light on the Microscopic Resonant Mechanism Responsible for Cavity-Mediated Chemical Reactivity," Nat. Commun. **13**, 7817 (2021).
[121]X. Li, A. Mandal, and P. Huo, "Cavity frequency-dependent theory for vibrational polariton chemistry," Nat. Commun. **12**, 1315 (2021).
[122]L. P. Lindoy, A. Mandal, and D. R. Reichman, "Resonant Cavity Modification of Ground-State Chemical Kinetics," J. Phys. Chem. Lett. **13**, 6580–6586 (2022).
[123]D. S. Wang, T. Neuman, S. F. Yelin, and J. Flick, "Cavity-Modified Unimolecular Dissociation Reactions via Intramolecular Vibrational Energy Redistribution," J. Phys. Chem. Lett. **13**, 3317–3324 (2022).
[124]M. Du, Y. R. Poh, and J. Yuen-Zhou, "Vibropolaritonic Reaction Rates in the Collective Strong Coupling Regime: Pollak–Grabert–Hänggi Theory," J. Phys. Chem. C **127**, 5230–5237 (2023).
[125]A. Mandal, X. Li, and P. Huo, "Theory of vibrational polariton chemistry in the collective coupling regime," J. Chem. Phys. **156**, 014101 (2022).
[126]P.-Y. Yang and J. Cao, "Quantum Effects in Chemical Reactions under Polaritonic Vibrational Strong Coupling," J. Phys. Chem. Lett. **12**, 9531–9538 (2021).
[127]J. Sun and O. Vendrell, "Suppression and Enhancement of Thermal Chemical Rates in a Cavity," J. Phys. Chem. Lett. **13**, 4441–4446 (2022).
[128]M. R. Fiechter, J. E. Runeson, J. E. Lawrence, and J. O. Richardson, "How Quantum is the Resonance Behavior in Vibrational Polariton Chemistry?" J. Phys. Chem. Lett. **14**, 8261–8267 (2023).
[129]M. C. Anderson, E. J. Woods, T. P. Fay, D. J. Wales, and D. T. Limmer, "On the Mechanism of Polaritonic Rate Suppression from Quantum Transition Paths," J. Phys. Chem. Lett. **14**, 6888–6894 (2023).
[130]L. P. Lindoy, A. Mandal, and D. R. Reichman, "Quantum dynamical effects of vibrational strong coupling in chemical reactivity," Nat. Commun. **14**, 2733 (2023).
[131]W. Ying and P. Huo, "Resonance theory and quantum dynamics simulations of vibrational polariton chemistry," J. Chem. Phys. **159**, 084104 (2023).
[132]D. Hu, W. Ying, and P. Huo, "Resonance Enhancement of Vibrational Polariton Chemistry Obtained from the Mixed Quantum-Classical Dynamics Simulations," J. Phys. Chem. Lett. **14**, 11208–11216 (2023).
[133]Y. Ke and J. O. Richardson, "Insights into the mechanisms of optical cavity-modified ground-state chemical reactions," J. Chem. Phys. **160**, 224704 (2024).
[134]Y. Ke and J. O. Richardson, "Quantum nature of reactivity modification in vibrational polariton chemistry," J. Chem. Phys. **161**, 054104 (2024).
[135]W. Ying and P. Huo, "Resonance theory of vibrational strong coupling enhanced polariton chemistry and the role of photonic mode lifetime," Commun. Mater. **5**, 110 (2024).
[136]W. Ying, M. A. D. Taylor, and P. Huo, "Resonance theory of vibrational polariton chemistry at the normal incidence," Nanophotonics **13**, 2601–2615 (2024).
[137]S. M. Vega, W. Ying, and P. Huo, "Theoretical Insights into the Resonant Suppression Effect in Vibrational Polariton Chemistry," J. Am. Chem. Soc. **147**, 19727–19737 (2025).
[138]T. E. Li, A. Nitzan, and J. E. Subotnik, "Collective vibrational strong coupling effects on molecular vibrational relaxation and energy transfer: Numerical insights via cavity molecular dynamics simulations," Angew. Chem. Int. Ed. **60**, 15533–15540 (2021).
[139]A. Shalabney, J. George, J. Hutchison, G. Pupillo, C. Genet, and T. W. Ebbesen, "Coherent coupling of molecular resonators with a microcavity mode," Nat. Commun. **6**, 5981 (2015).
[140]H. A. Kramers and W. Heisenberg, "Über die streuung von strahlung durch atome," Z. Phys. **31**, 681–708 (1925).
[141]P. Hänggi, P. Talkner, and M. Borkovec, "Reaction-rate theory: fifty years after Kramers," Rev. Mod. Phys. **62**, 251–341 (1990).
[142]A. P. Fidler, L. Chen, A. M. McKillop, and M. L. Weichman, "Ultrafast dynamics of CN radical reactions with chloroform solvent under vibrational strong coupling," J. Chem. Phys. **159**, 164302 (2023).
[143]L. Chen, A. P. Fidler, A. M. McKillop, and M. L. Weichman, "Exploring the impact of vibrational cavity coupling strength on ultrafast CN + c-C6H12 reaction dynamics," Nanophotonics **13**, 2591–2599 (2024).
[144]K. Hirai, J. A. Hutchison, and H. Uji-i, "Recent Progress in Vibropolaritonic Chemistry," ChemPlusChem **85**, 1981–1988 (2020).